Republic of Iraq
Ministry of Higher Education
and Scientific Research
University of Babylon
College of Engineering
Mechanical Engineering Department

INVESTIGATION OF THE PULSE FLOW IN A WAVY CHANNEL FILLED WITH KEROSENE FUEL

A Research Submitted to the
College of Engineering / University of Babylon in
Partial Fulfillment of the Requirements for the Degree of
Higher Diploma in Engineering / Mechanical Engineering /
Fuel and Power

By

Ameer Kareem Salho Jraah.

Supervised By

Assist. Prof. Dr. Hameed K. Hamzah

2022 A.D.

بسم الله الرحمن الرحيم

(قَالُواْ سُبْحَانَكَ لاَ عِلْمَ لَنَا إِلاَّ مَا عَلَّمْتَنَا

إِنَّكَ أَنتَ الْعَلِيمُ الْحَكِيمُ)

صدق الله العلي العظيم

سورة البقرة ﴿32﴾

Certification

I certify that this research entitled **" Investigation of The Pulse Flow in a Wavy Channel Filled with Kerosene Fuel "** has been prepared by "***Ameer Kareem Salho***" under my supervision at the department of Mechanical Engineering, College of Engineering, University of Babylon as a partial fulfillment of the requirements for the Degree of Higher Diploma of Science in Mechanical Engineering / Fuel and Power.

I recommend that this research be forwarded for examination in accordance with the regulation of the University of Babylon.

Signature

Assist. Prof. Dr. Hameed K. Hamzah

Department of Mechanical Engineering

College of Engineering

University of Babylon/Iraq

Data: / / 2022

Dedication

To

My dear father, God is the longest in his life

My mother, God is the longest in her life

My dear brother and the flowers of my life, my sisters

My best friend in my life Ahmed

I dedicate my modest effort.

Ameer Kareem Salho.

Acknowledgments

(In The Name of Allah, The Gracious, The Merciful)

(Thanks to Allah for his guidance and help)

I wish to express my sincere thanks and deep gratitude to my supervisor ***Assist. Prof. Dr. Hameed K.*** *Hamzah for their invaluable help, advice, and encouragement during the various stages of the present work.*

I would like also to submit my thanks to all staff members of the Department of Mechanical Engineering at the University of Babylon, Head of the Department ***Assist. Prof. Dr. Samer Mohammed****, for his constructive contribution to this study.*

My deepest thanks, love, and gratitude for all of my family. This study would not have been completed without their love and continuous support.

Deep thanks to my friend ***Ahmed Mohammed Al-Obaidi*** *to help me and stay beside me to the end and supporting me.*

Ameer Kareem Salho

/ / 2022

Abstract

The heat transfer of kerosene fuel was studied numerically within wave shape channel with pulsing flow. The study focused on knowing of fuel effect in the amount of heat transfer depending on the physical properties of the fuel in the wave channel.

The Computational fluid dynamics module at COMSOL Multiphysics was used in this study, and it was based on the Finite element method used to solve the Partial differential equation that govern the problem such as momentum, continuity, and energy. Several variables were investigated in this study, including the values of Reynolds numbers (200 ≤Re≤ 800), as well as several values of Strouhal Numbers (0 ≤St≤ 0.15) were investigated. Also, different wave shapes channel was used, including the waves number (0 ≤β≤ 8) as well as different values of the wave amplitude (0 ≤α ≤0.3). In the current study, it can be concluded that there was an improvement in the amount of heat transfer for the fuel used when increasing the Strouhal Numbers with an increasing in Reynolds number, which is the increasing leads to an increase ($Nu_{\bar{\tau}}$) and this is lead to improve the heat transfer rate. and it was also observed that two increasing the number of waves of the wavy channel, the surface area of the channel increases, and this leads to improve in the heat transfer values, as the values of ($Nu_{\bar{\tau}}$= 107.82) were observed at (β=4,Re=800,α=0.2,St=0.15,t=118) and the percentage of enhancement are (1.53662), while the value of ($Nu_{\bar{\tau}}$= 124.26) becomes at the same properties(Re=800,α=0.2,St=0.15,t=118), but at the value of (β=8) and the percentage of enhancement are(1.923306). It also noticed that the values of heat transfer improvement in an obvious increase when increasing the amplitude of the wave, because the increase in the amplitude of the wave also leads to an increase in the surface area of the channel and this leads to an increase in the amplitude of the wave, therefore the percentage of

enhancement are (2.663) when the value of ($Nu_{\bar{\tau}}$= 146.2) at the wave amplitude (α=0.3) and (Re=800).

Nomenclature

Symbol	Meaning	Unit
Nu_0	No wavy Nusselt number	
Nu	local Nusselt number	----
Pr	Prandtl number.	----
Re	Reynolds number.	----
$Nu_{\bar{x}}$	Space Averaged Nusselt number	----
St	Strouhal number	----
$Nu_{\bar{\tau}}$	Time Average Nusselt number	----
T	Temperature	°C
c_p	Specific heat factor	J/kg. °C
H	Height of channel	m
x_i	inlet position to wavy channel	m
x_o	outlet position to wavy channel	m
A	The wave amplitude of pulsating flow.	m
u_{in}	Inlet velocity	m/s
u, v	x-y velocity components	m/s
t	Time	s
q	Heat transfer rate	W
k	Thermal conductivity coefficient	W/m. °C
h	Convection heat transfer coefficient	W/m^2. °C

Greek Symbols

Symbol	Meaning	Unit
α	Amplitude of wave channel	----
θ	dimensionless temperature	----
τ	Dimensionless time	----
β	Number of waves	----
Γ	The period of pulsing flow.	----
ρ	Density	(kg/m^3)
μ	Dynamic viscosity	(Pa.s)
ν	Kinematic viscosity of the fluid	m^2/s

Subscripts

Symbol	Description
cond.	Conduction
conv.	Convection
eff	Effectiveness
in	Input
h	Hot surface

Abbreviations

Symbol	Description
CFD	Computational Fluid Dynamic

Contents

CHAPTER ONE

INTRODUCTION

Chapter One: Introduction

1.1 General Introduction

The improvement in heat exchanger performance in recent years has been to meet the industry's requirement for premium heat transfer quality. Corrugated surfaces in heat exchangers, on the other hand, have attained their maximum heat transfer enhancement. The need for more advanced heat transfer technologies has grown rapidly. On the coolant and fuel side, typical heat transfer fluids with low thermal conductivities (such as water, oil, ethylene glycol, Diesel, kerosene and gasoline) are seen as a major barrier to enhancing heat exchanger performance [1].

The study of pulsing flow under diverse geometrical circumstances is of wide interest in a variety of scientific domains. [2–5]. Heat transfer under pulsing flow is commonly observed in many industrial applications from an engineering standpoint. The relevance of pulsing flow in current industrial applications is shown by its use in the cooling system in gas turbine engines, stirling engines and in small or large engineering scales such as electronic devices. In ocean environments, the pulsing flow of convective coolant in nuclear power plants is uniform. Pulsing flow and heat transfer play a major role in the thermo-hydraulic study of nuclear reactors and safety assessment [6].

1.2 Different Flow Types

Different forms of flow can be found with distinct features in different issues and environments:

1. Steady and Unsteady flow.
2. Uniform and non-uniform flow.
3. Flow in one, two, and three dimensions.
4. Rotational or irrotational flow.

5. Laminar or turbulent flow.

1.2.1 Pulsing flow: General and Physics Concept

Womersley flow, also known as pulsing flow in fluid dynamics, is a flow having periodic changes. John R. Womersley (1907–1958) derived the flow profiles in his research on blood flow in arteries. Pulsatile flow is most commonly seen in Chordata animals' circulatory systems, but it may also be found in engines and hydraulic systems as a result of rotating machinery pushing the fluid [7].

The pulsing flow has a sinusoidal shape and oscillates around the temporal-averaged flow velocity, resulting in a single-harmonic velocity waveform in the pulsing flow.

The pulsing flow is one of the types of flow in which the value of the velocity changes with time and this change is a fixed wave function during time as in Figure (1-1) where it shows the change in the value of the velocity during time [8].

The pulsing flow can be represented by different functions such as the sinusoidal function, Square-wave pulsing flow, semi sinusoidal-wave, half semi sinusoidal-wave as in Figure (1-2) where the researcher used various forms of functions [9].

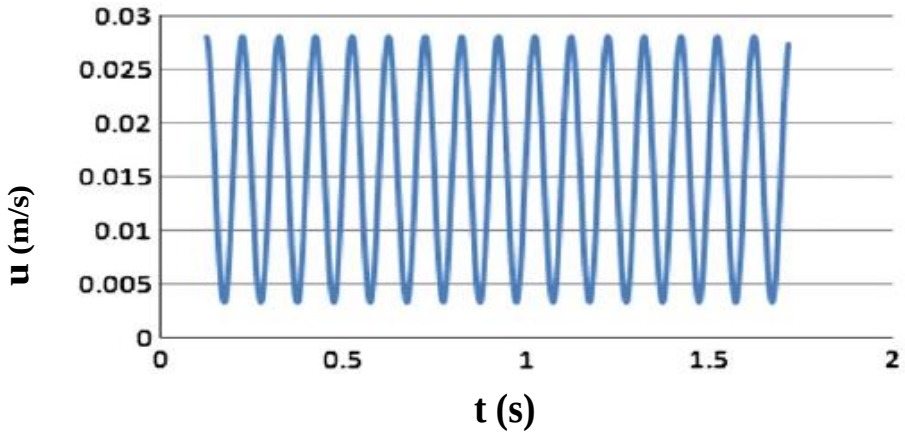

Figure (1- 1) Pulsing flow [8] .

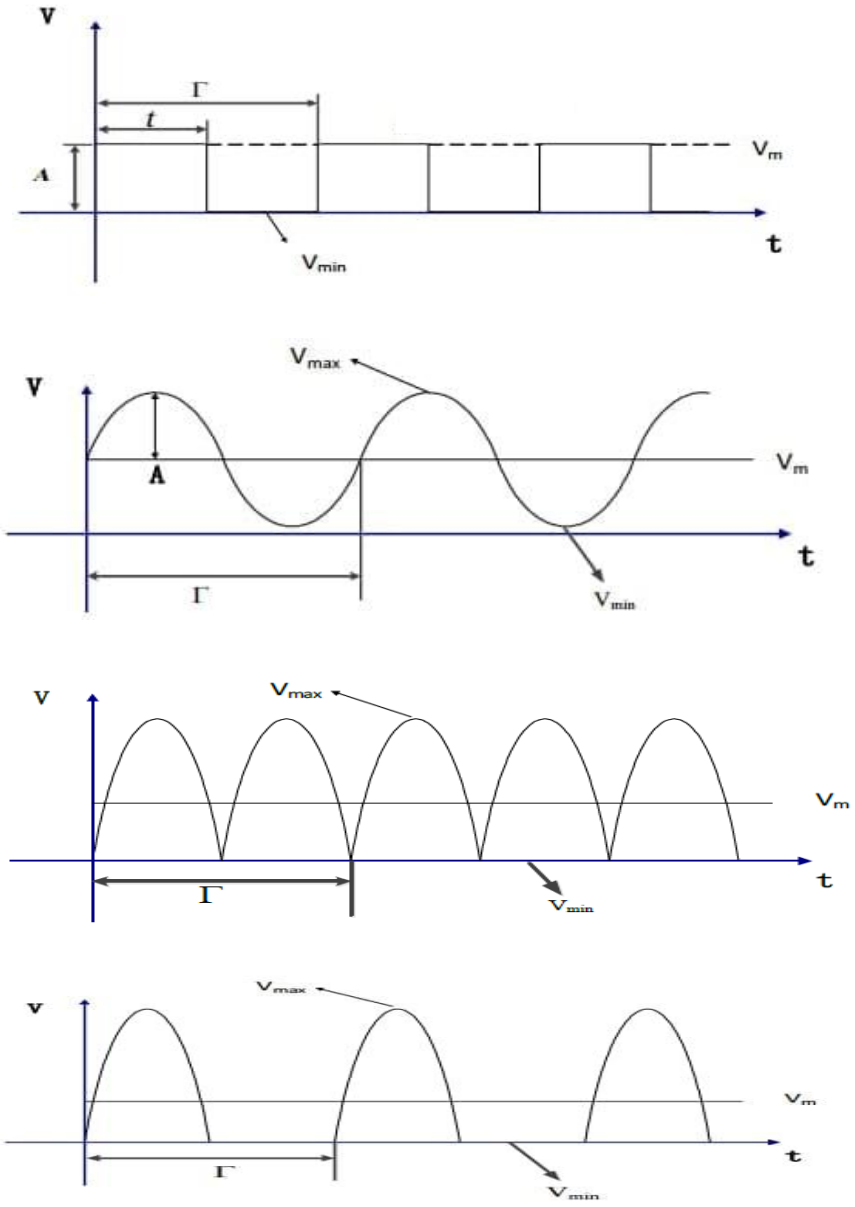

***Figure (1- 2) Pulsing flow function types*[9] .**

1.3 Applications of Pulsing Flow.

Pulsing flow has a wide range of applications in a variety of fields:

1.3.1 Pulsing flow in the human body

To circulate blood and exchange air throughout the body (respiratory system). within the human body. The arteries transport blood throughout the body. Veins, on the other hand, gather deoxygenated blood from all throughout the body and transport it to the heart. Valve mechanisms, or the

opening and closing of valves at certain time intervals, regulate blood circulation fully, resulting in a pulsing flow of blood [7].

1.3.2 Pulsing combustor

The burning of solid, liquid, and gaseous fuel occurs periodically in a pulsing combustor. An input valve, a combustion chamber, and a resonance tube for expelling gases are the main components. Through the valves, air and fuel enter the combustion chamber, which is subsequently ignited with the assistance of a spark plug. As the pressure of the gases rises due to combustion, valves close and the gases travel towards the exhaust. The vacuum formed in the combustion chamber causes valves to open, allowing fuel-air combustion to occur, which is ignited by the heated environment. Furthermore, without the use of a spark plug, some exhaust gases flow back into the combustion chamber. The combustion process is repeated by varying the air and fuel flow on a regular basis, as shown in Figure (1-3) [10].

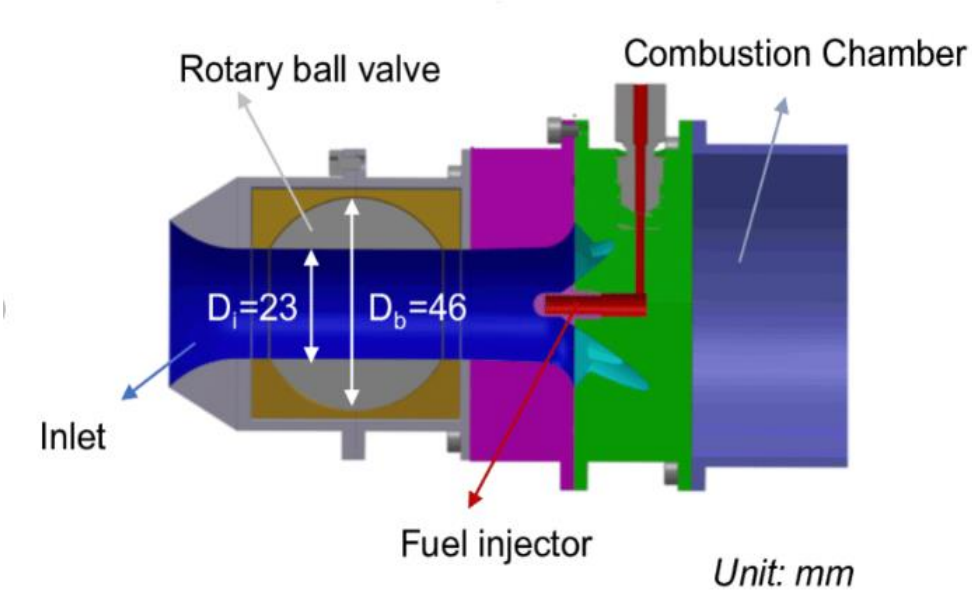

Figure (1- 3) Pulsing combustor [10].

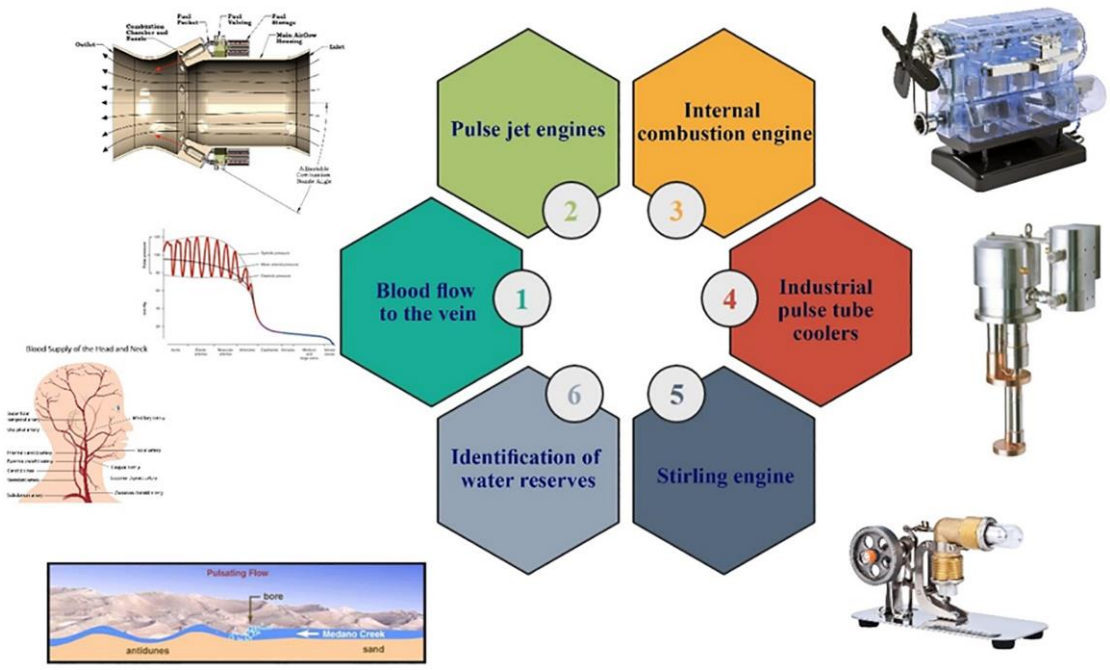

Figure (1- 4) Pulsing application [11].

1.4 Classification of Heat Transfer Improvement

There are many techniques for enhancing heat transfer processes. This techniques are classified as either passive or active. Even though it generates a pressure decrease, passive approaches do not require direct external energy input. A summary in Table (1-1) of the different methods or devices in each of these two groups[12] .

Table (1- 1) Types of heat transfer enhancers [12].

Passive Techniques	**Active Techniques**
Treated surfaces	Mechanical aids
Rough surfaces	Surface vibration
Extended surfaces	Fluid vibration
Displaced enhancement devices	Electrostatic fields
Swirl flow devices	Injection

Coiled tubes	Suction
Surface tension devices	Jet impingement

1.5 Wave Channel

Wavy channels represent an effective means in the process of improving heat transfer, as these channels provide a larger surface area than flat channels, which increases the area of heat exchange. Wavy channels have recently been used in many applications of heat exchangers, as the curvature of the surfaces in these channels contributes to the process of taking on vorticity, which in turn improves the thermal performance of the heat exchangers. This method is one of the effective heat improvement methods. As shown in Figure (1-5), some researchers used wavy channels with a sinusoidal function, as the shapes of these channels and the way they are organized differed. While some researchers used corrugated channels as in Figure (1-6) .

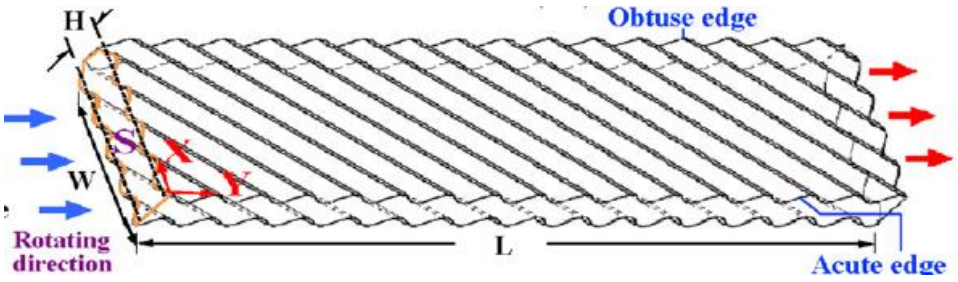

(a)

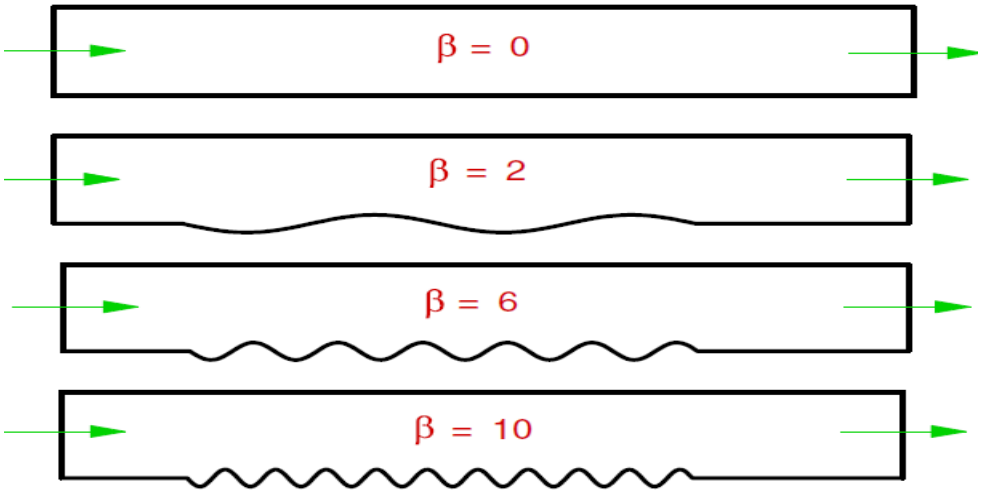

(b)

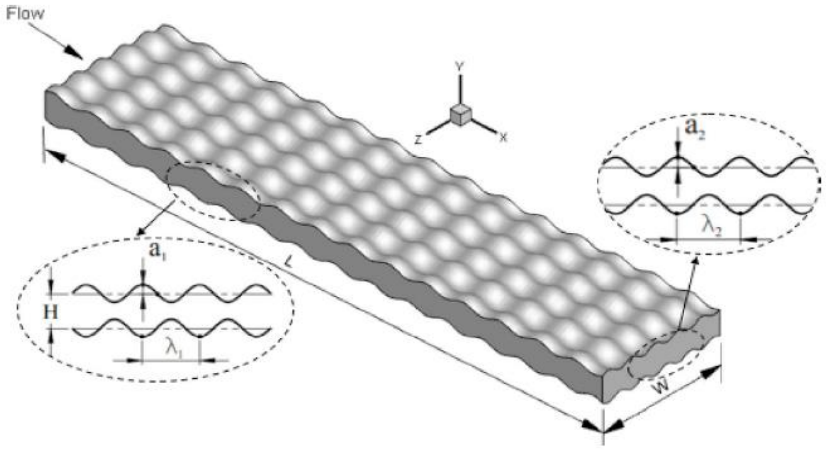

(c)

Figure (1- 5) (a) Two opposite skewed sinusoidal wavy walls [13]. (b), (c) wavy channel[14], [15].

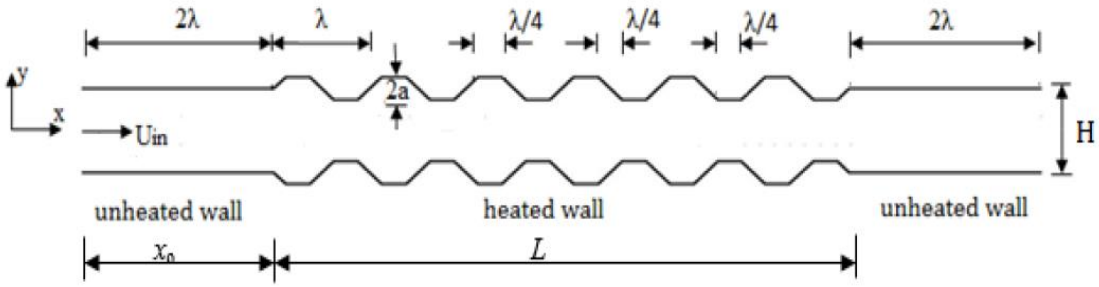

Figure (1- 6)Trapezoidal corrugated channel [16].

1.6 Working Fluid

In this study, the focus was on the use of fuel as working fluid, and this reflect the many applications in which the wavy channel can be used to transport through them. Where kerosene fuel was used as a model for the study.

1.6.1 Kerosene

Kerosene is a flammable hydrocarbon liquid generated from petroleum. It is commonly utilized as a fuel in both aircraft and domestic appliances.

In a highly refined version known as RP-1, kerosene is frequently used to power jet engines of airplanes (jet fuel) and certain rocket engines. It's also a popular cooking and lighting fuel.

Kerosene is a polluting fuel, according to the World Health Organization, and "governments and practitioners should immediately stop encouraging its domestic usage." Kerosene smoke includes a high concentration of hazardous particle matter.[17]**.**

Table (1-2) Properties of kerosene [17].

Property	**Symbol**	**Value**
Prandtl number	Pr	31.4
Thermal conductivity (*W/m K)*	k	0.145
Kinematic viscosity *(*m^2/s*)*	ν	2.71
Specific heat *(kJ/(kg K))*	c_p	2.01
Density*(*kg/m^3*)*	ρ	840

1.7 Objectives of the present work

The main objective of this study was to find out the best case for improving the rate of heat transfer in the wavy channel using pulsing flow. Three important cases were used and comparing the effect on heat transfer. These three cases were used with three values of Reynolds number ($200 \leq Re \leq 800$), where these three cases first include the extent of the effect of changing Strouhal number ($0 \leq St \leq 0.15$) on heat transfer and flow. As well as three values of wavy number were used ($0 \leq \beta \leq 8$) and observing the extent of the effect of changing the number of wavy numbers at each Reynolds number and its impact on the improvement of heat transfer and pulsing flow. And finally, three values of wavy amplitude were used, namely ($0 \leq \alpha \leq 0.3$), all the variables were used for kerosene fuel, where this numerical method was studied through COMSOL Multiphysics program.

CHAPTER TWO

LITERATURE REVIEW

Chapter Two: Literature Reviews

2.1 Introduction

Pulsing flow has attracted the attention of many researchers from view point of its effect on heat transfer. There are many numerical and experimental studies that investigate the heat transfer performance of pulsing flow through the different geometries. Since internal forced convection phenomena has great importance in numerous engineering applications, studies about pulsing flow and heat transfer in channels, ducts and tubes came into prominence.

In this chapter, the latest developments, results and research related to this study are mentioned and reviewed. Thermal management systems including pulsing and wave channel heat sinks are accomplished of removing high fluxes of heat from small surfaces professionally. Various heat transfer enhancement techniques have been accepted in the literature as following:

2.2 Literature reviews

2.2.1 Pulsing Flow

Jafari et al.2013 [18] investigated the effects of pulsing flow on forced convection in a corrugated channel using the Lattice Boltzmann Method, which is a variation of the Boundary Fitting Method. When Prandtl number equals 3.103, they do the study of various Reynolds numbers (50, 100, and 150). Temporal variations of streamlines, isotherms, relative pressure drop, and Nusselt number are supplied for appropriate dimensionless groups. It was revealed that the variability in heat transfer rate as a function of Strouhal number has an extremum peak. They found that the variation of heat transfer rate according to Strouhal number has an extremum peak. In this extremum

value pulsing velocity gradient has the best effects on heat transfer rate and heat transfer rate start to drop for higher frequencies.

Harun et al.2017 [19] studied numerically the heat transfer process under the influence of pulsing flow inside an undulating channel. The temperature of the channel wall was constant. Reynolds number was used in the study with different values between (200 and 800) Strouhal numbers were between (0.05, 0.15, 0.25). The focus of the study was based on the difference in the structure of the channel with the pulsing flow. The study proved that the pulsing flow greatly enhanced the heat transfer process.

Zhang et al. 2018 [9] studied numerically pseudoplastic fluid flow and heat transfer process under the influence of pulsing flow inside the multi-channel heat sink. Various pulsing flow functions were used, where three types of pulsing flow functions were used, namely square wave, sinusoidal wave and shaped wave trapezoidal. It was found that all forms of flow the pulsed wave was better in the process of heat transfer than the constant flow. Also, through the results of the study, it was proved that the sine wave was the best type in the process of heat transfer among other types of pulse functions.

Yang et al. 2018 [20] studied numerically the effect of polygonal channels of different shapes on pulsing flow as well as heat transfer methods. The study was applied to a number of polygonal channels of different shapes with multiple angles, including (30^o, 45^o, 60^o, 90^o) as well as at the value of (Aspect ratio=2) and ($10000 \leq Re \leq 60000$). The secondary flows were studied as well as the values of (Nu) in these polygonal channels for both the pulse flow and the stationary flow. The study proved that the pulsing flow affected the longitudinal flow and the transverse flow with completely different values. The study also proved that the values of (Time average Nusselt number) in the case of pulsing flow are much higher than their values for

constant flow. This, in turn, depends on the angle, the larger it is, the greater the amount (Time average Nusselt number). Also, the increase in the wide (Re) improves the heat transfer process.

Hamid et al.2019 [21] studied numerically of non-Newtonian fluid under the influence of pulsing flow within an undulating channel using Lattice Boltzmann method. Several values of the pulsing amplitude ($0 \leq$ pulse amplitude ≤ 0.35) were used, as the value of the pulsing amplitude at zero represents the constant flow. Also, several values of the Reynolds number (50,100,150,200) were used, with a fixed value taken from the Strouhal number (0.25). The pulsing amplitude as well as the Reynolds number were identified as the main variables influencing the pulsing flow behavior. As the pulsing amplitude of oscillating flow increases, velocity profiles show a bigger difference at various periodic time points. This difference for power law indices n = 1.4 varies from 6% at $A_{pulse} = 0.05$ up to 35% at $A_{pulse} = 0.35$. In contrast, velocity profiles tend to unify under each non-Newtonian regime as the pulsing amplitude becomes smaller towards steady state ($A_{pulse} = 0.05$). Shear thickening fluid allows more volumetric flow rate as well as higher peak velocity than the shear thinning fluid at each pulsing amplitude studied.

Kurtulmus and Sahin 2019[22] investigated experimentally the heat transfer transfer process under the influence of a pulsing flow within a sinusoidal channel and a comparison of the results of pulsing flow with constant flow. Heat transfer experiments were carried out under conditions in which the heat flow values were constant, as well as the used Strouhal number between (0.11 to 2.07) and the value of the Reynolds number between ($4*10^3$ to $7*10^3$). They showed that the use of pulsing flow has a very high efficiency in the case of turbulent flow in the sinusoidal channel.

Yu et al.2020 [23] experimentally studied of the process of mass transfer and fluid flow using sodium carboxymethylcellulose solution inside

pipes with undulating walls and under the influence of pulsing flow as well as constant flow. The researchers used in their study the method particle image velocimetry (PIV). It has been shown that increasing the concentration of the used solution hinders (slows) the performance of the mass transfer of the solution, but the mass transfer can be improved by increasing the capacity of the corrugated tubes. Through the study, it was noted that the mass transfer increases with the pulsing flow.

Davletshin et al.2020 [24] investigated experimentally the heat transport and kinematic structure of constant and pulsing airflow via a span-wise rib. The value of the frequency forcing was between (0–30) Hz, and the value of the amplitude is 0.5. When comparing the study of the stationary flow condition with the case of pulsing flow, it was found that the pulsing flow has a clear effect in improving heat transfer. Velocity and turbulence parameter profiles are shown at a number of typical points along the separation zone. The dynamics of the kinematic structure of pulsing flows are characterized using parameter profiles in various phases of forced flow pulsations. The distributions of the transverse velocity component correspond well with the distributions of the heat transfer coefficient across the wall in the rib wake.

2.2.2 Wavy Channel

Chang et al. 2010 [13] studied the heat transfers in a radially rotating furrowed channel with two opposing walls were explored experimentally using full-field Nusselt number (Nu) data over two wavy walls augmented by skewed sinusoidal waves. Although the static wavy channel has been demonstrated to be an effective heat transfer enhancement measure, as a first attempt for turbine cooling research, Nu scans were acquired over the entire rotational leading (stable) and trailing (unstable) walls using infrared

thermography, which proved extremely advantageous due to its ability to examine the rotating buoyancy effects.

Heidary and Kermani 2012 [14] investigated numerically the heat transfer and flow field analysis in a wavy channel coupled to a porous Gas Diffusion Layer. The temperature of the fluid entering the channel (T_{in}) was selected to be lower than the temperature of the channel walls (T_w). Numerous numerical evaluations are performed across a range of Reynolds numbers Re_H: $100 \leq Re_H \leq 1000$, wave numbers: $0 \leq \beta \leq 10$, wave amplitudes: $0 \leq \alpha \leq 0.3$, and Darcy numbers Da: $0.1 \leq Da \leq 0.001$. Depending on the duct and flow rate Re_H, simulations reveal that heat transfer in channels can improve by up to 100% depending on the duct (β),(α), and flow rate (Re_H).

Nandi and Chattopadhyay 2013 [8] examined numerically the unstable laminar fluid flow and heat transfer within a two-dimensional wavy microchannel due to a sinusoidally varying velocity component at the intake. While maintaining a constant temperature on the channel walls, the flow evolved thermally and hydrodynamically. The simulation was conducted in the laminar domain for Prandtl number 7 for water and Reynolds values ranging from 0.1 to 100. In compared to continuous flow in a wavy channel, it was observed that imposing sinusoidal velocity at the intake may significantly improve heat transfer performance for a variety of amplitudes (0.2, 0.5, 0.8) and frequencies (1, 5, 10).

Jafari et al 2015. [25] investigated the influence of single-walled carbon nanotubes on convection heat transfer in a corrugated channel with a pulsing velocity profile. Strouhal number and amplitude of pulsating velocity are explored for various Reynolds numbers in the ranges 0.05–0.25 and 0–0.5, respectively (50, 100, and 150). The intended results were computed and provided as time-averaged Nusselt number and relative pressure decreased throughout the course of a pulse duration. The results

established that the use of single-walled carbon nanotube particles in convectional channels were a viable technique for increasing convection rate and reducing pressure loss.

Zhu et al. 2016 [26] investigated a wavy-tape insert prototype for enhancing pipe heat transfer. The core of a straight pipe was fitted with wavy tape. In the thermal entrance zone with isothermal boundary conditions, full-scale simulations with $200 \leq Re \leq 2200$ are performed. The maxima overall heat transfer enhancement ratio of wavy-tape $(Nu_{wavy}/Nu_{no\ wavy})/(f_{wavy}/ f_{no\ wavy})^{1/3}$ inserts was 1. 82. The parametric experiments were being conducted to determine the effect of the amplitude and width of wavy-tapes on the thermal-hydraulic performance of pipes, compared the heat absorption rate of wavy-tape inserted pipe to that of hollow pipe using the identical pumping power consumption criterion. The former was bigger by 120–178 percent than the latter.

Ramgadia and Saha 2016 [27] evaluated numerically fully developed flow and heat transfer using an asymmetric wavy-walled design. Periodic boundary conditions were employed to simulate completely developed flow and heat transfer in three distinct geometries created using three-phase shift angles (φ) between two opposed heated walls. The essential Reynolds number of unsteadiness is highest for the symmetric ($\varphi = 180^o$) wavy-walled channel. The flow was similarly intricate in all three geometries, but the asymmetric geometry with 0^o phase-shift revealed the largest asymmetry in the flow near the centerline.

Harikrishnan and Tiwari 2019[15] studied numerically a sinusoidal undulating channel and the effect of heat transfer properties with the number of corrugations. The study dealt with three-dimensional numerical investigations, and numerical calculations were made for the study using (ANSYS Fluent) program. The study mainly depended on changing the

channel structure by changing the number of ripples as well as changing the corrugates amplitude 0.1 ≤wave amplitudes≤ 0.3 values and different values of Reynolds numbers 2000 ≤Re≤ 4000. The flow within normal channels was also compared with the flow characteristics within channels with different corrugates. Studies have shown that the heat transfer process improves in the case of the use of undulating channels.

Yuan et al. 2020 [28] investigated experimentally and numerically the irregular micro-wavy channels and the effect of heat transfer as well as mass transfer within the used channels. They studied the effect of Reynolds number ≤2000 Re≤10000 and the peak deviation position on the thermo-hydraulic process inside the micro-channels used in the study. The results of the researcher showed that the heat transfer of divergent wavy channel with peak position far is good compared with convergent wavy channel of microchannels. It matched the theoretical results compared with expiring and they were identical to the process of heat and mass transfer.

2.2.3 Channel With Fuel Flow.

Zhaohui Liu et al.2012 [29] investigated experimentally of subcooled flow boiling heat transfer characteristics a kerosene kind hydrocarbon fuel was investigated in an electrically heated horizontal tube with an inner diameter of 1.0 mm, in the range of heat flux: 20–1500 kW/m2, fluid temperature: 25–400 C, mass flux: 1260–2160 kg/m2 s, and pressure: 0.25–2.5 MPa. It was noticed propose that the nucleate boiling heat transfer mechanism is dominant, as the heat transfer performance are dependent on heat flux imposed on the channel, rather than the fuel flow rate. It was found that the wall temperatures along the test section were kept constant during the fully developed subcooled boiling (FDSB) of the non-azeotropic hydrocarbon fuel. After the onset of nucleate boiling, the temperature differences between the inner wall and bulk fluid begin to decrease with the

increase of heat flux. Experimental results show that the complicated boiling heat transfer behavior of hydrocarbon fuel is profoundly affected by the pressure and heat flux, especially by fuel subcooling. A correlation of heat transfer coefficients varying with heat fluxes and fuel subcooling was curve fitted. Excellent agreement is obtained between the predicted values and the experimental data.

2.3 Summary of Literature Review

Table (2- 1) summary of Pulsing flow

Ref. No.	Authors	Type of channel	Type of Study	Conclusions
18	Jafariet al.2013	Corrugated	Numerically	It is observed that amplitude of oscillating velocity has a linear increase on heat transfer rate and the role of oscillating amplitude becomes more important in the extremum value of Strouhal number.
19	Harun et al.2017	Wavy Channel	Numerically	They concluded that heat transfer enhancement is not significant and the effect of Reynolds number was limited for the Strouhal number of St=0.05. This situation changes with increasing Strouhal number (St); heat transfer enhancement gets better and the role of the Reynolds

				number becomes more dominant.
9	Zhang et al. 2018	Manifold microchannel heat sink	Numerically	They noticed that heat transfer enhancement by pulsating flow was attributed to two scenarios which were the continuously developing characteristics of the flow and the occurrence of strong secondary flows or reverse flows. The pulsing flow was always in the developing stage and can never reach a developed status, which makes the secondary flow or reverse to be easily induced
20	Yang et al. 2018	Various ribbed channels	Numerically	Pulsing flow results in higher pressure loss, friction factor ratio increases with pulsing frequency and amplitude. For Re=40000 and A=0.2, the thermal performance was increased by 39% at the optimal frequency for the 90^{o} ribbed channel, which is 8.3% for the 60^{o} ribbed channel and 4.9% for the 30^{o} ribbed channel. The 45^{o} ribbed channel shows no enhancement of thermal

				performance compared to a steady flow.
21	Hamid et al.2019	Corrugated channel	Numerically	As the pulse amplitude of oscillating flow increases, velocity profiles show bigger differences at various periodic time points. This difference for n = 1.4 varies from 6% at A_{pulse} = 0.05 up to 35% at A_{pulse} = 0.35. In contrast, velocity profiles tend to unify under each non-Newtonian regime as the pulse amplitude becomes smaller towards steady-state (A_{pulse} = 0.05). Shear thickening fluid allows more volumetric flow rate as well as higher peak velocity than the shear-thinning fluid at each pulse amplitude studied.
22	Kurtulmus and Sahin 2019	Sinusoidal channels	Experimental	The heat transfer ratio, η was obtained as 1.5 which is the maximum value in the case of the sinusoidal channel for the Reynolds number of $Re=4*10^3$ and the Strouhal number of St=1.03.

23	Yu et al.2020	wavy-walled tubes	Experimental	Phase shift phenomenon was observed in wavy-walled tubes under pulsating flow. The phase difference increases as St and amplitude of tube increase, which was unaffected by the wavelength, polymer concentration, and oscillatory fraction.
24	Davletshin et al.2020	Rib	Experimental	Experimental data on heat transfer and kinematic structure of the separated flow past a spanwise rib in a channel were obtained for steady and pulsing flow modes. In general, the forced flow pulsing were shown to enhance heat transfer compared to the steady flow case. The most pronounced augmentation of local heat transfer (up to three times compared to the steady flow at the same average flow rate) is observed in the near wake of the rib

Table (2- 2) Summary of wavy channel

13	Chang et al. 2010	Radially rotating furrowed channel	Experimental	They found that with the full Nu scans collected from the rotational leading and

		with two opposites skewed sinusoidal wavy walls		trailing wavy walls, the location dependent heat transfer modifications from the stationary references were disclosed. The trailing Nu elevations are triggered from the developed flow region along the obtuse edge and extended in both obtuse-toacut and upstream directions as Ro increases. On the leading wall, the evident Nu recovery from the worst heat transfer scenarios at Ro above 0.06 also emerges along the obtuse edge of the developed flow region and expands as similar as that on the trailing wall when Ro was increased from 0.06 onward.
14	Heidary and Kermani 2012	wavy channel linked to a porous domain	Numerically	1-It was observed that the construction of wavy walls (with the waves in the perpendicular direction to the main flow) can significantly enhance the heat exchange between the wall and the flow. 2-The heat exchange between the wavy wall and

				the core flow strongly depends on the wall wave amplitudes. For example, at α=0.3 and β=10, the Nusselt number can enhance by a factor of 2 to 2.5. Heat exchange with the porous wall also increases by a lower factor, ≈1.2.
8	Nandi and Chattopadhyay 2013	Wavy micro-channels	Numerically	The pulsing at inlet was found to enhance heat transfer with reduced pressure drop even at low Re. Thermal development lengths in wavy microchannels were also estimated.
25	Jafari et al 2015.	Corrugated channel	Numerically	The effects of oscillation amplitude and Strouhal number (dimensionless frequency) of pulsing velocity profile were investigated for different Reynolds numbers. The results show that pulsing velocity plays a considerable role in the configuration of flow and thermal fields in the wavy channel.
26	Zhu et al. 2016	wavy-tape insert	Numerically	They observed that for a typical wavy-tape inserted pipe, the global Nusselt

		configuration for pipe		number was enhanced by 2.74–3.54 folds with a 4.22–7.32 times increase in friction factor compared with the hollow pipe. The overall heat enhancement ratio g ups to 1.82. The wavy tape induces significant swirl flow inside the pipe. Particularly, pairs of tangential vortices were generated on the flanks.
27	Ramgadia and Saha 2016	Wavy-walled design	Numerically	The flow asymmetry has been found to be the most for the asymmetric channel having $\varphi = 0^{O}$. It was observed that the most asymmetric geometry with $\varphi = 0^{O}$ generates higher Nusselt number but accompanied by relatively high pressure drop penalty in comparison to other geometries. However, the TPF is found to be the highest for $\varphi = 0^{O}$ shifts because of the relative increase in heat transfer was quite high that of friction factor for this geometry. The higher streamwise velocity

				fluctuations and the corresponding higher correlations between velocity and temperature fields for asymmetric geometry with $\varphi = 0^{O}$ was responsible for higher momentum transport thus leading to the highest heat transfer among all geometries.
15	Harikrishnan and Tiwari 2019	sinusoidal wavy channel with secondary corrugations	Numerically	Nusselt number and friction factor were found to be higher for streamwise corrugated channels followed by secondary corrugated and spanwise corrugated channels. An increase in streamwise wave amplitude in the secondary corrugated channel increases Nu as well as f whereas an increase in spanwise wave amplitude results in a decrease of both Nu as well as f. Moreover, both heat transfer as well as friction factor decrease with an increase in the number of waves for given amplitude in the spanwise direction.

28	Yuan et al. 2020	wavy micro channels	Numerically	They concluded, Nu and PEC of wavy microchannels with a wavelength of 5.0 mm increased with the increase in Reynolds number. Both the Nu and PEC of MCH-41 were larger than that of MCH-41 and MCH-05, respectively. The divergent wavy cavity effectively enhanced the mass and heat transfer performance

Table (2- 3) summary of fuel with channel

29	Zhaohui Liu et al.2012	1 mm diameter channel	Experimental	They concluded that was the fuel subcooling was found to affect the heat transfer of hydrocarbon fuel strongly. The boiling heat transfer at the same fluid temperature was suppressed due to the increase of subcooling as pressure increased. A higher heat transfer coefficient was attained at higher fuel temperature owing to the fuel subcooling decrease. In order to predict the heat transfer coefficients at the FDSB region for different pressures, heat fluxes, and fluid temperatures, a correlation of heat transfer

				coefficient h with fuel subcooling DTsub and heat flux q was curve fitted. Excellent agreement was obtained between the predicted data and the experimental data.

CHAPTER THREE

Numerical Analysis

Chapter Three: Numerical Analysis

3.1 Introduction

In this chapter, the numerical model and all its details were reviewed, starting with building the geometer of the wavy channel and setting the boundary conditions on a model, then clarifying the equations governing the model.

The use of fuel within these channels was also explained and the thermal properties of kerosene fuel that was studied and reviewed.

The study focused on using the (CFD) to represent the pulsing flow entering the wavy channel, and it clarified the effect of channel dimensions on thermal performance.

3.2 Model description

In this study, it has been used a two-dimensional wave channel and studied the pulsing flow through it. This channel has a known dimension where (H) represents the height of the channel and (20H) represents the length of the channel as shown in the Figure (3.1).

The channel consists of three regions, the first region represents the entrance region, which is a flat and its length is (3H), and the second region is the region of the wavy channel, which wavy with sinusoidal function as in the following equation [19]:

$$y = \alpha \left[\sin\left(2\pi\beta \frac{x-x_i}{x_o-x_i}\right)\right] \quad \ldots (3.1)$$

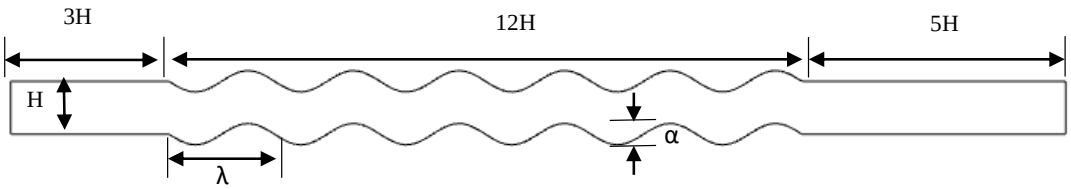

Figure (3- 1) Schematic view of channel.

3.2.1 Assumptions

The following assumptions were used in the numerical simulations:

1-Flow is pulse i.e., transient with sinusoidal function.

2- The thermophysical characteristic of working fluid remain constant.

3- The gravity and radiation modes of heat transfer are ignored.

4- Single phase, 2D, laminar, and incompressible fluid flow were considered.

5- The flow is fully developed

6- kerosene is Newtonian fluid.

3.2.2 Dimensionless Equation:

The non-dimensional variables that will be used as follows [30]:

$$(U,V) = \frac{(u,v)}{u_o} \quad \ldots (3.2)$$

$$(X,Y) = \frac{(x,y)}{H} \quad \ldots (3.3)$$

$$\theta = \frac{T - T_{in}}{T_{wall} - T_{in}} \quad \ldots (3.4)$$

$$\tau = \frac{tu_o}{H} \quad \ldots (3.5)$$

$$Re = \frac{\rho u H}{\mu} \quad \ldots (3.6)$$

$$Pr = \frac{C_p \mu}{k} \quad \ldots (3.7)$$

$$P = \frac{p}{\rho u_o} \quad \ldots (3.8)$$

non-dimensional form of governing equations becomes:

Continuity equation:

$$\frac{\partial U}{\partial X} + \frac{\partial V}{\partial Y} = 0 \quad \ldots (3.9)$$

Momentum equation:

In x-direction

$$\frac{\partial U}{\partial \tau} + U\frac{\partial U}{\partial X} + V\frac{\partial U}{\partial Y} = -\frac{\partial P}{\partial X} + \frac{1}{Re}\left(\frac{\partial^2 U}{\partial X^2} + \frac{\partial^2 U}{\partial Y^2}\right) \quad \ldots (3.10)$$

In y-direction

$$\frac{\partial V}{\partial \tau} + U\frac{\partial V}{\partial X} + V\frac{\partial V}{\partial Y} = -\frac{\partial P}{\partial Y} + \frac{1}{Re}\left(\frac{\partial^2 V}{\partial X^2} + \frac{\partial^2 V}{\partial Y^2}\right) \quad \ldots (3.11)$$

Energy equation:

$$\frac{\partial \theta}{\partial \tau} + U\frac{\partial \theta}{\partial X} + V\frac{\partial \theta}{\partial Y} = \frac{1}{RePr}\left(\frac{\partial^2 \theta}{\partial X^2} + \frac{\partial^2 \theta}{\partial Y^2}\right) \quad \ldots (3.12)$$

Where **(y)** represents the normal direction to surface so, the general equation become [19]:

$$\text{Local:Nu} = \left(\frac{-H}{T_{wall} - T_{in}}\right)\left((\partial T/\partial n)|_{\text{Bottom Wall}} + (\partial T/\partial n)|_{\text{Top Wall}}\right) \ldots (3.13)$$

Where (n) represent normal direction to surface.

$$\text{Space averaged: } \text{Nu}_{\bar{x}} = \frac{1}{(x_o - x_i)}\int_{x_s}^{x_e} Nu dx \quad \ldots (3.14)$$

$$\text{Space and period averaged: } Nu_{\bar{\tau}} = \frac{1}{\tau_p}\int_0^{2\pi} Nu_{\bar{x}} d\tau \quad \ldots (3.15)$$

3.2.3 Boundary condition

Nusselt number will be calculated to represent the thermal performance of the channel. Nusselt number represents the ratio of heat flux by the fluid when heat is transferred through the fluid layer by convection when the fluid is moving to heat flux by the fluid when heat is transferred through the fluid layer by conduction when the fluid is motionless.

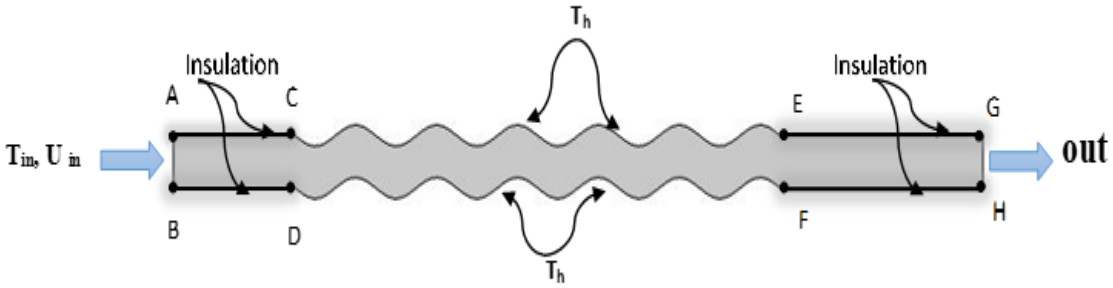

Figure (3- 2) Boundary domain.

3.2.4 Dimensionless boundary conditions

Table (3- 1) value of dimensionless boundary condition

location	Momentum	Energy
A-B	$U(Y,\tau) = \frac{3}{2}u_0(1-(Y-1)^2)[1+\alpha \sin(2\pi St\tau)]$	θ =0
A-C	No slip U=0, V=0	Thermal insulation θ=0
B-D	No slip U=0, V=0	Thermal insulation θ=0
C-E	No slip U=0, V=0	θ =1
D-F	No slip U=0, V=0	θ =1
E-G	No slip U=0, V=0	Thermal insulation θ=0
F-H	No slip U=0, V=0	Thermal insulation θ=0
G-H	P_O=0	Outlet condition

$$U(Y,\tau) = \frac{3}{2}u_0(1-(Y-1)^2)[1+\alpha \sin(2\pi St\tau)] \text{ [18]} \quad \ldots (3.16)$$

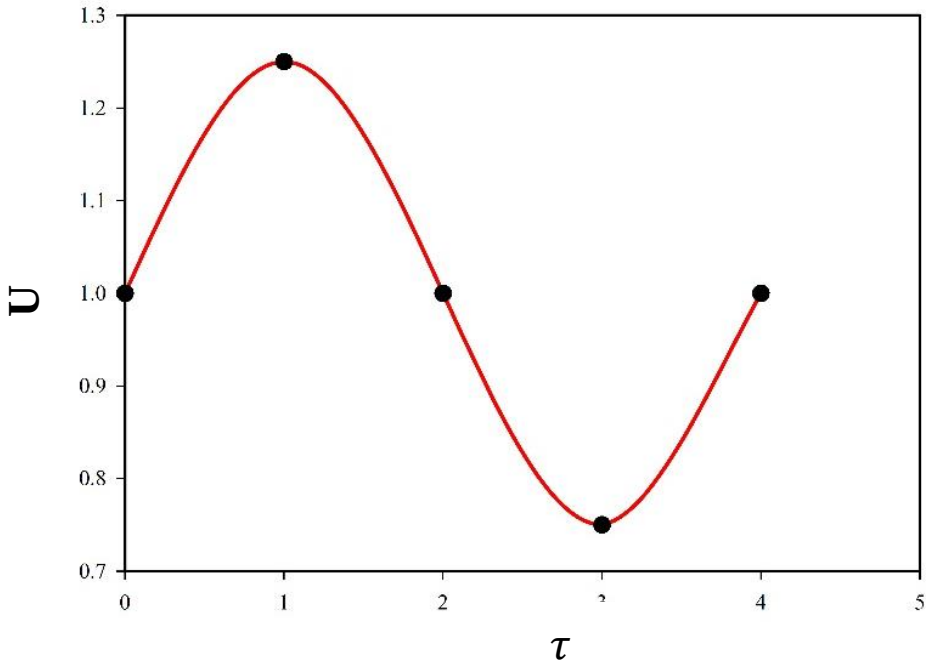

Figure (3- 3) Pulsing inlet velocity.

Where (St) is the Strouhal number which represents non-dimensional frequency and it is defined as [19]**:**

$$St = \frac{fH}{u_0} \quad \ldots (3.17)$$

The percentage of improvement in Nusselt number value can be found by using the following relationship:

$$Enhancement = \frac{Nu_{wave} - Nu_o}{Nu_o} \quad \ldots (3.18)$$

3.3 CFD modelling

All the above equations have been solved using the software package (COMSOL Multiphysics 5.5).

3.3.1 Mesh and grid generation

A mesh is a small discrete cell representation of a bigger geometric region. Meshes are frequently employed to solve partial

differential equation solutions and to produce computer graphics. A mesh divides space into components (or cells or zones) across which equations may be solved, resulting in an approximation of the answer over a wider domain. Within a model, element boundaries might be limited to sit on internal or exterior boundaries. Higher-quality (better-shaped) elements have higher numerical qualities, where "better" is defined by the general governing equations and the specific solution to the model instance.

There are two sorts of two-dimensional cell forms that are used in this study. Which are triangle and quadrilateral.

a- Triangle

This cell form has three sides and is one of the most basic types of mesh. It is usually quick and simple to generate a triangular surface mesh. It is especially prevalent in unstructured grids.as shown in figure (3-4).

b- Quadrilateral

This cell form is a simple four-sided one, as seen in the illustration. It is most commonly encountered in organized grids.

Quadrilateral components are often not allowed to be or become concave, as shown in Figure (3-4).

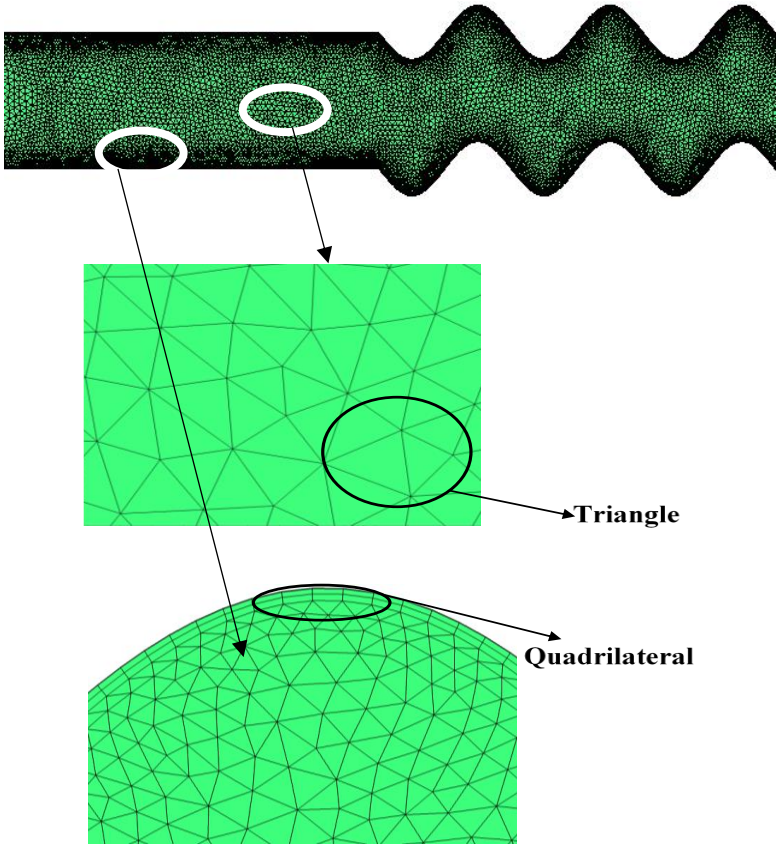

Figure (3- 4) Types of mesh used in this study.

In this study finer mesh used, as this type is considered to be one of the most accurate types of mesh. If a more accurate solution is determined more rapidly, a mesh is regarded to be of higher quality. Accuracy and speed are odds. Reducing the size of the meh usually improves accuracy but raises the computational cost and time. Accuracy is determined by the overall number of components as well as the form of individual elements. The speed of each iteration increases (linearly) with the number of elements, and the number of iterations required is determined by the local solution value and gradient in relation to the form and size of local elements.

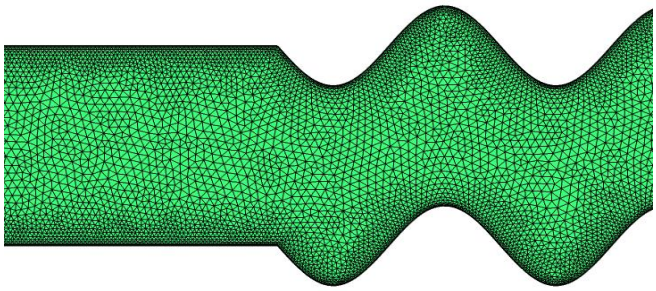

Figure (3- 5) Type of mesh using in this study.

3.4 Grid generation and grid independence test

Any independent variables, where (m) denotes the number of iterations (velocity, temperature or pressure). To validate the correctness of the calculated findings, a grid-independent test is now required. Five grid resolutions were used to accomplish this, as shown in Table (3-3). The time average Nusselt number at (β=6, α=0.2, Re=200, Pr=31.4, and St=0.25). The grid with (39066) give lower value of error (4.7%). As shown in figure (3-4)

Table (3- 2) Grid independent test

Grid	Maximum face size	Number of elements	Nusselt Number
G1	0.5	4142	29.57334
G2	0.4	4220	29.23271
G3	0.2	7276	31.84605
G4	0.08	39066	49.19556
G5	0.06	67106	51.55

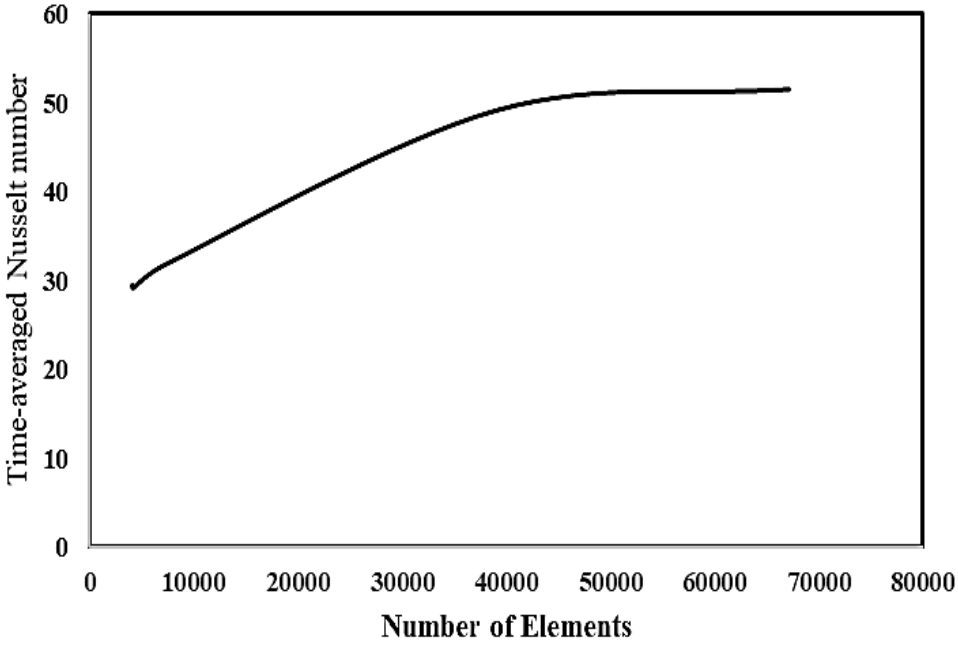

Figure (3- 6) Grid independent test.

CHAPTER FOUR

Results And Discussion

Results and Discussion

4.1 Introduction

The numerical results are explained in this chapter and the improvement in heat transfer and flow through the wavy channel is discussed.

The numerical study focused on the use of a number of variables on the flow as well as on the structure of the channel three important cases were used and comparing the effect of heat transfer. Where these three cases were used with three values of Reynolds number ($200 \leq Re \leq 800$), where these three cases first include the extent of the effect of changing Strouhal number ($0 \leq St \leq 0.15$) on heat transfer and flow. As well as three values of wavy numbers were used ($0 \leq \beta \leq 8$) and observing the extent of the effect of changing the number of wavy numbers at each Reynolds number and its impact on the improvement of heat transfer and pulsing flow. And finally, three values of wavy amplitude were used, namely ($0 \leq \alpha \leq 0.3$), all the variables were used for kerosene fuel, where this numerical method was studied through a program COMSOL Multiphysics.

4.2 Validation

To ensure that the numerical findings of the current work are accurate, which is achieved using COMSOL Multiphysics software, the outcomes of the present code were compared with the results of other researchers. The numerical solution was validated with the published work of **Zontul et al. (2017)** [19] Where this study was included laminar pulsing flow in wavy channel. The comparison of the solution program used in this study with **Zontul et al. (2017)** [19] results as illustrated in Figure (4-1).

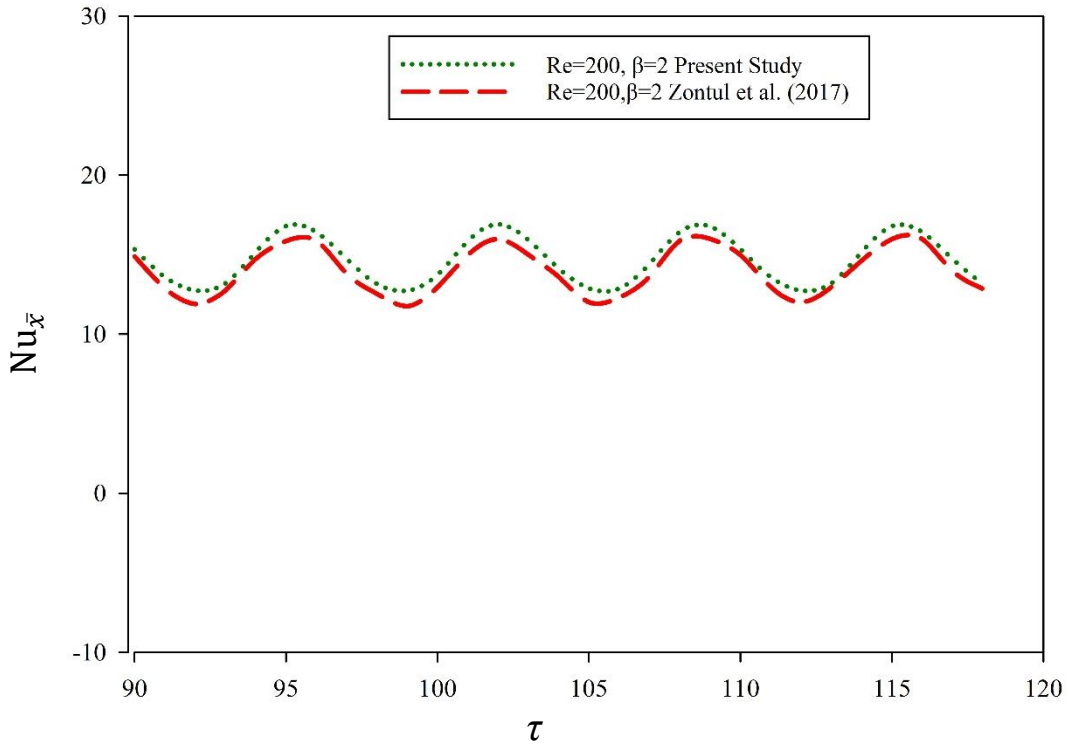

Figure (4- 1) Comparison between the current study software results and the study of Zontul et al. (2017), space Nusselt number ($Nu_{\bar{x}}$) with time at different wavy number and Re = 200.

τ	**Present Study**
60	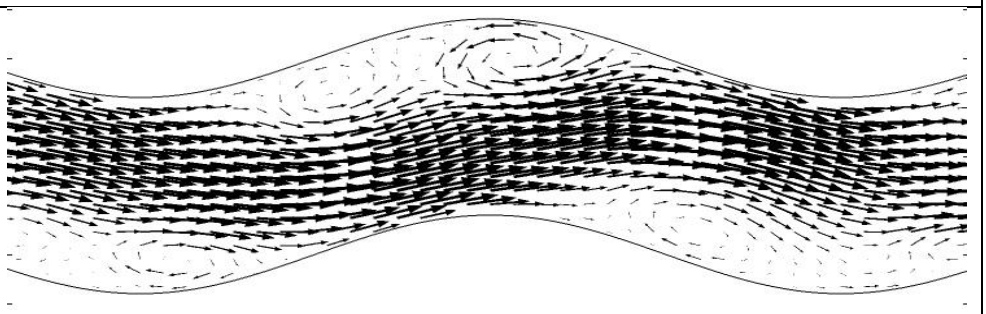
60	***Study of Zontul et al. (2017)***
	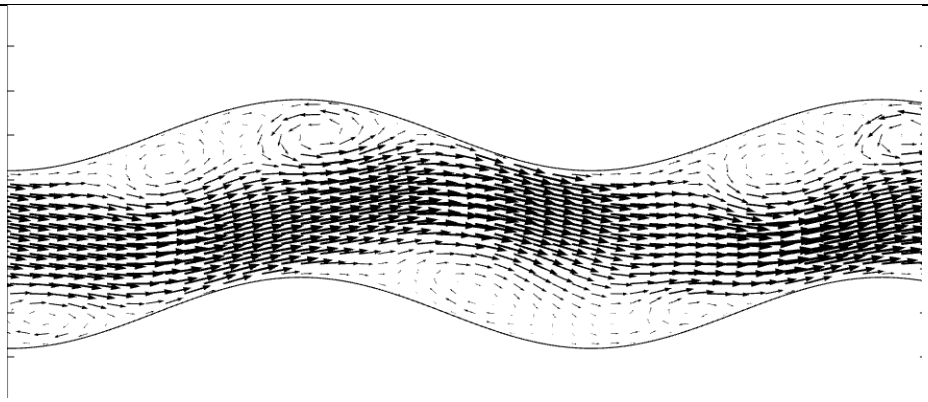

Figure (4- 2) Comparison between the current study software results and the study of Zontul et al. [19], Arrow surface at Re=400, St=0.15.

4.3 Numerical Results for Kerosene Fuel

4.3.1 Effect of Strouhal Numbers

4.3.1.1 Time Average Nusselt Number

Figures (4- 3 and 4- 4) show the relationship between Time-averaged Nusselt number ($\overline{Nu_{\tau}}$), Reynolds numbers (Re) and different Strouhal Numbers (St), through the first figure it was noticed that the relationship between ($\overline{Nu_{\tau}}$) with (Re) at different values of (St) it has noticed that with an increasing in the value of (Re) the values of ($\overline{Nu_{\tau}}$) increased and so does this increase be at its highest value with an increment (St). Also, it has

noticed that it reaches its highest value at (Re=800) as well as at the highest value of (St=0.15), where ($Nu_{\bar{\tau}}$=66.457) at (St=0) and ($Nu_{\bar{\tau}}$= 75.9307) at (St=0.15). Therefore, the heat transfer enhancement will be at its best value (St=0.15) and it makes a big difference, while it is not possible to notice a big difference in the heat transfer rate between the values of (St=0, St=0.05) even by increasing (Re), it did not notice a significant change in the amount of heat transfer.

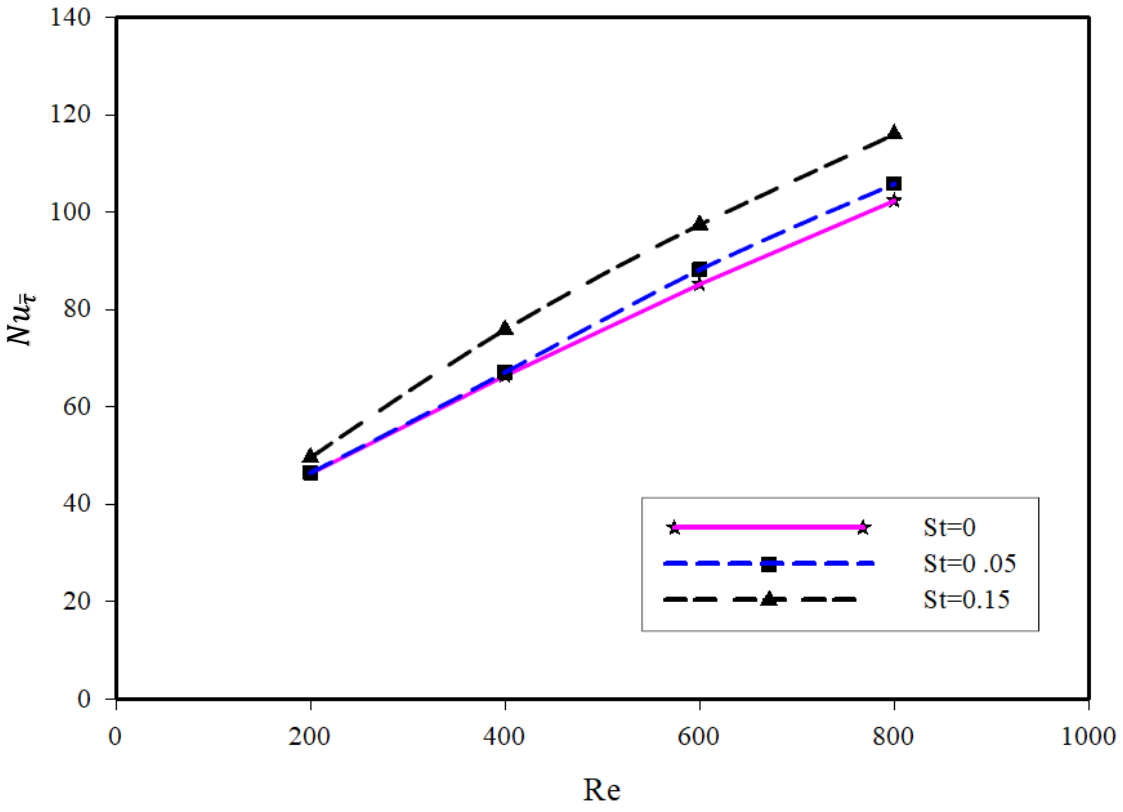

Figure (4- 3) the relation between Time-averaged Nusselt number ($Nu_{\bar{\tau}}$) with Reynolds numbers (Re) at different Strouhal Numbers (St).

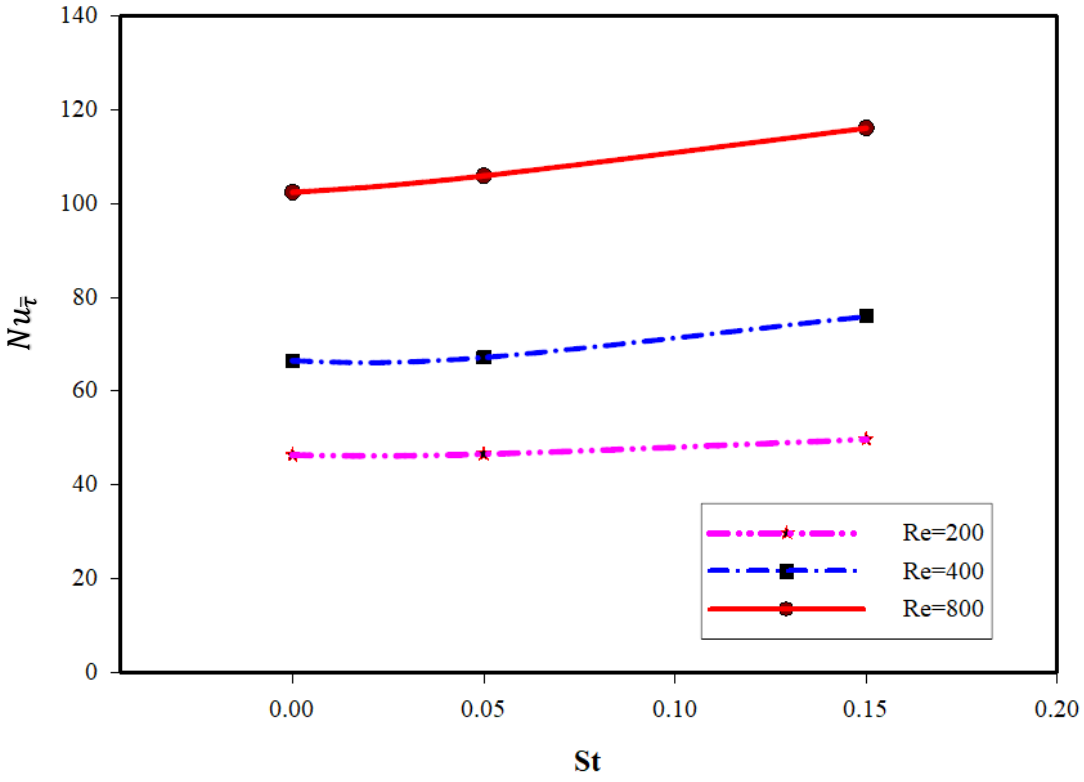

Figure (4- 4) the relation between Time-averaged Nusselt number ($Nu_{\bar{\tau}}$) with Strouhal Numbers (St) at different Reynolds numbers (Re).

4.3.1.2 Space averaged Nusselt Number

Figure (4-5) shows the relationship between space averaged Nusselt number ($Nu_{\bar{x}}$), different Strouhal numbers (St) with time, the variation of space averaged Nusselt number for wavy walls is demonstrated in Figure (4-5) As it is seen in the figure there is a strong relationship between pulsation dimensionless velocity (U) profile and the Nusselt number. Just like a pulsation of inlet flow, the Nusselt number reduces at the deceleration phase and it increases at the acceleration phase. It is obviously seen in figure (4-5) when Strouhal numbers (St) are equal to 0.15 the smallest value of the Nusselt number is higher than the steady case. But for the Strouhal number (St) the value of 0.05, the Nusselt number becomes lower than the steady case when the inlet velocity decreases; even so, the space and time-averaged Nusselt number is still higher than the steady case.

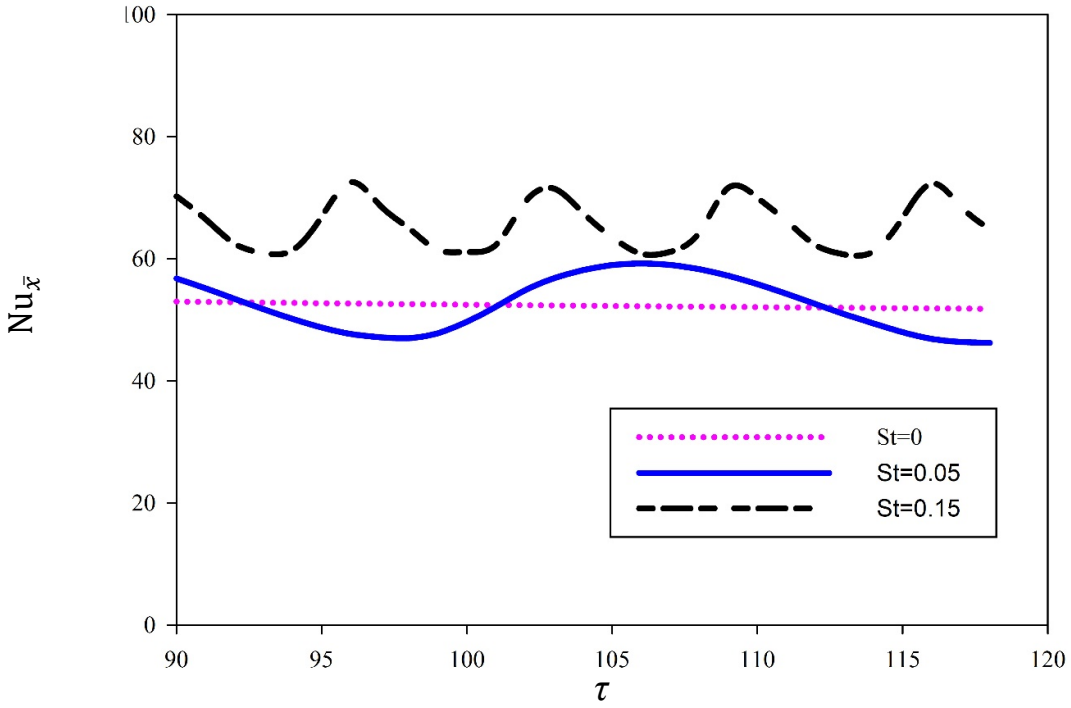

Figure (4- 5) the relation between variation of the space Nusselt number ($Nu_{\bar{x}}$ ***) with time at different Strouhal numbers (St) and Re = 400.***

4.3.1.3 Local Nusselt Number

Figures (4- 6,4-7 and 4-8) show the relationship between local Nusselt number (Nu), arc length (x), and different value of Strouhal Numbers (St) at Re=400, β=4, Pr=31.4, α= 0.2 and different time. From the figure, it was noticed that the value of (Nu) increased with (St) where (Nu=3.5-65) at (St=0) and this increasing continue to be between (3.9 to 97) at (St=0.15).

So, whenever (St) increase, (Nu) increase, Therefore, the pulse flow increases.

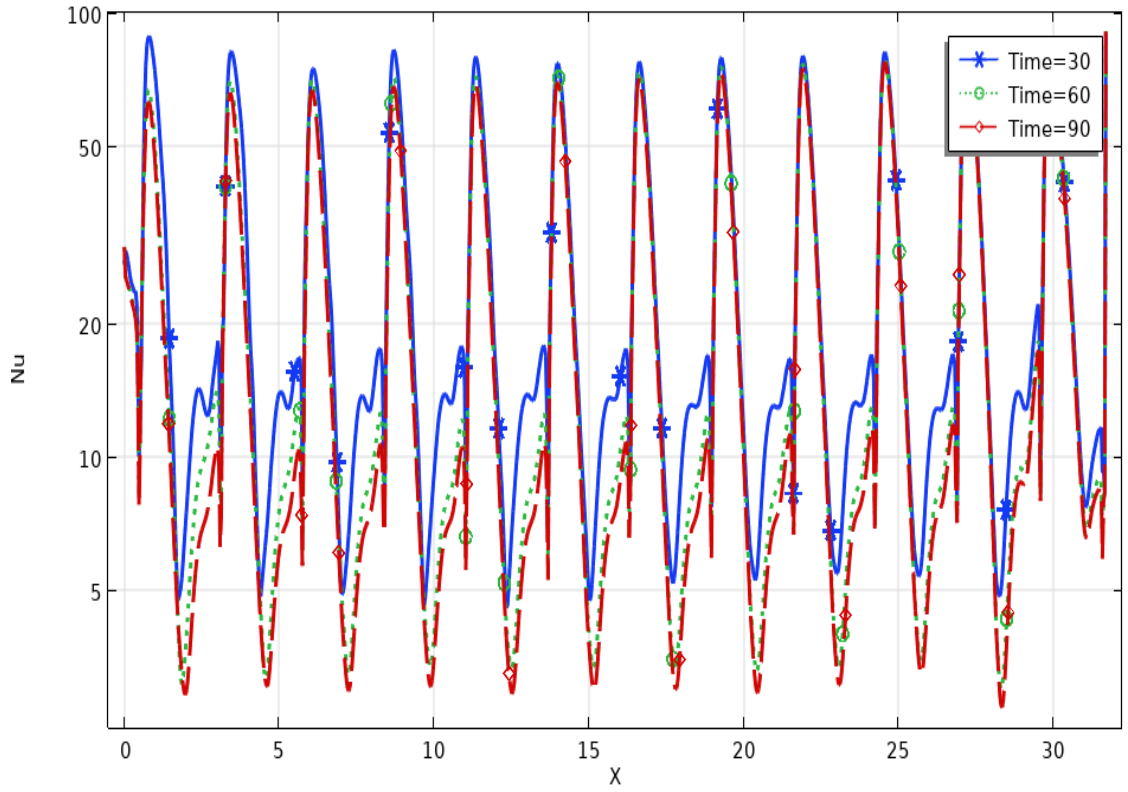

Figure (4- 6) the relation between Nusselt number distribution along the wall channel under pulsing flow with St = 0 at different time.

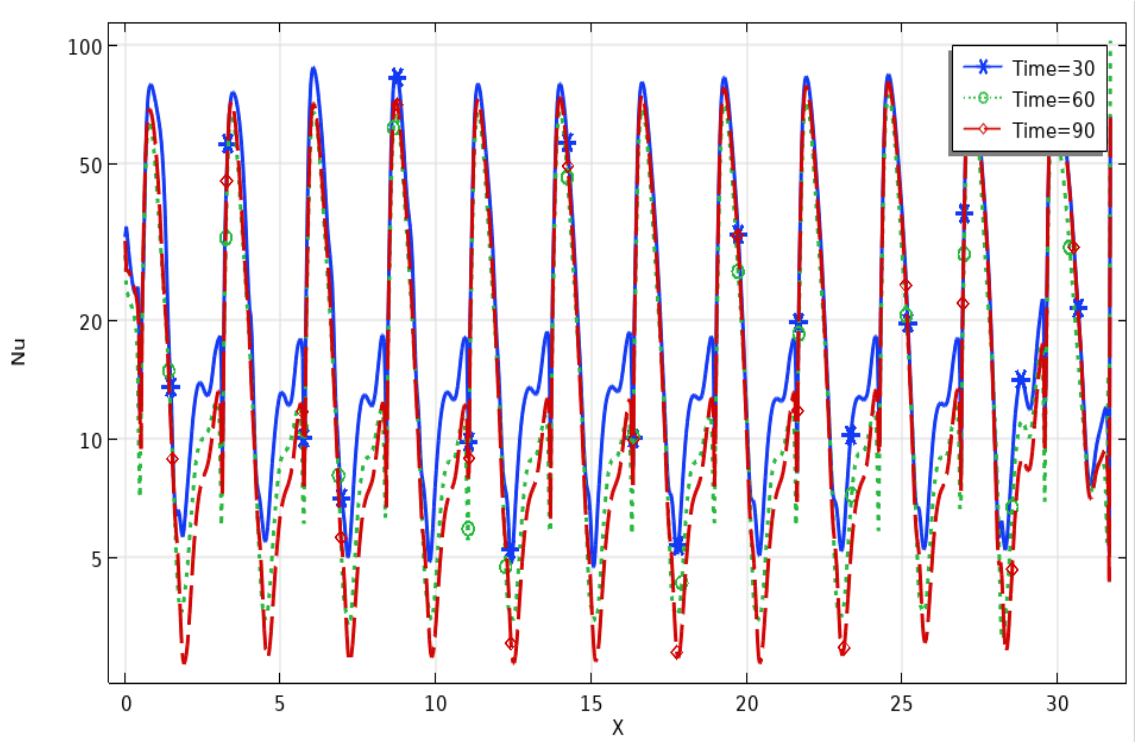

Figure (4- 7) the relation between local Nusselt number distribution along the wall channel under pulsing flow with St = 0.05 at different time.

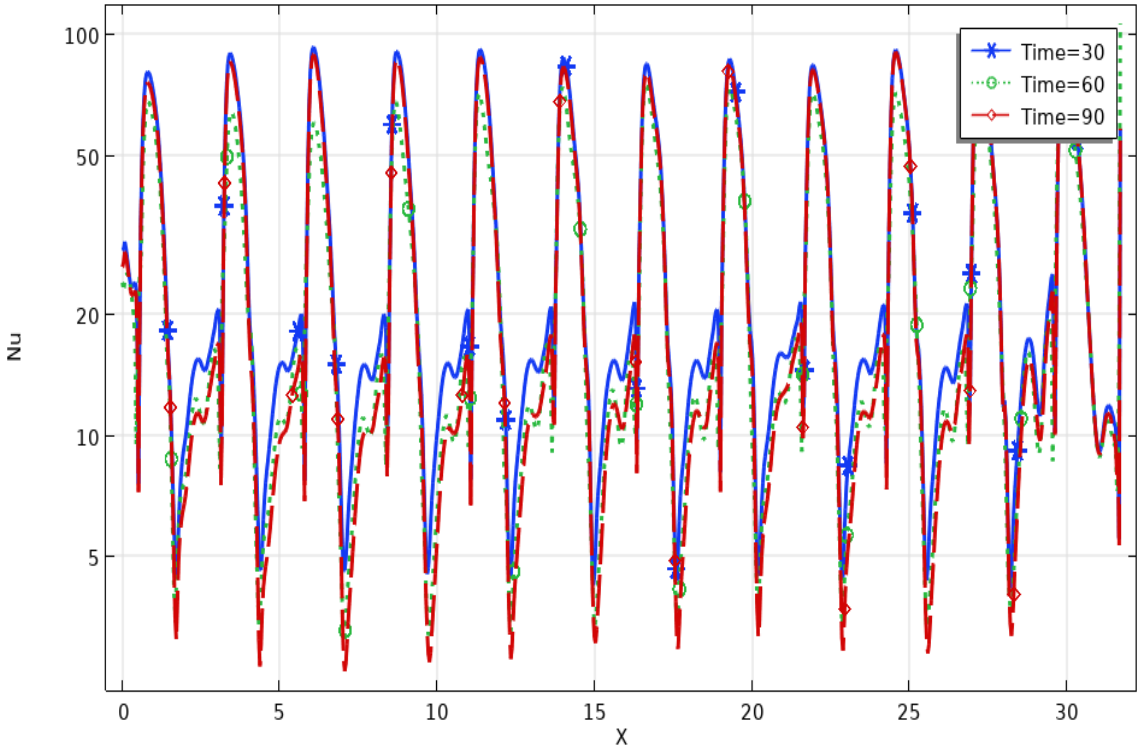

Figure (4- 8) the relation between local Nusselt number distribution along the wall channel under pulsating flow with St = 0.15 at different time.

4.3.2 Effect of wave number

4.3.2.1 Time Average Nusselt Number and Space Average Nusselt Number.

Figures (4-9 and 4-10) show the relationship between Time-averaged Nusselt number ($Nu_{\bar{\tau}}$) and wavy number (β) with at different Reynolds numbers (Re). Through the figure, it was noticed that the amount of ($Nu_{\bar{\tau}}$) increased with the increasing of (β) as well as with the increasing of the amount of (Re). But it was noticed that this increase is large between the value of wavy number (0, 4) but when incrementing the values of (β) over (4), it has been observed that the increment is small.

As a result, it was discovered that increasing (β) improves heat transfer significantly.

Figure (4-11) show the relationship between space average Nusselt number ($Nu_{\bar{x}}$), time at different value of wavy number (β), and a constant value of (Re = 400). It was noticed that the value of ($Nu_{\bar{x}}$) is constant with time but

increases with increasing value (β). And, it was noticed the amount of flow remains constant with time but increases with increase the value of (β). The value of ($Nu_{\bar{x}}$) continue increasing with increase (β). It's also noticed its value when (β=4) and above increasing but with little value.

Through figure (4- 12) it was noticed that at the value of (β=0), the flow is near to be smooth flow, but when (β=4 and above) is near to be the same value, as the flow is pulsing for all values of (β).

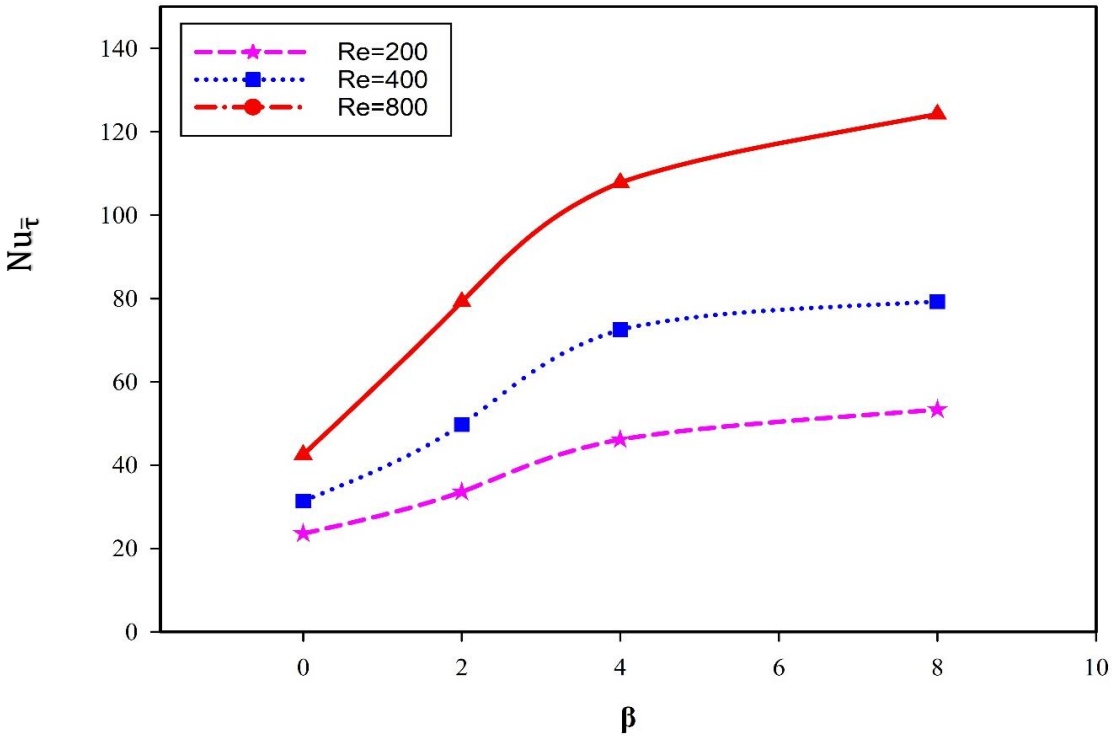

Figure (4- 9) the relation between Time-averaged Nusselt number ($Nu_{\bar{\tau}}$) with wavy number (β) at different Reynolds numbers (Re).

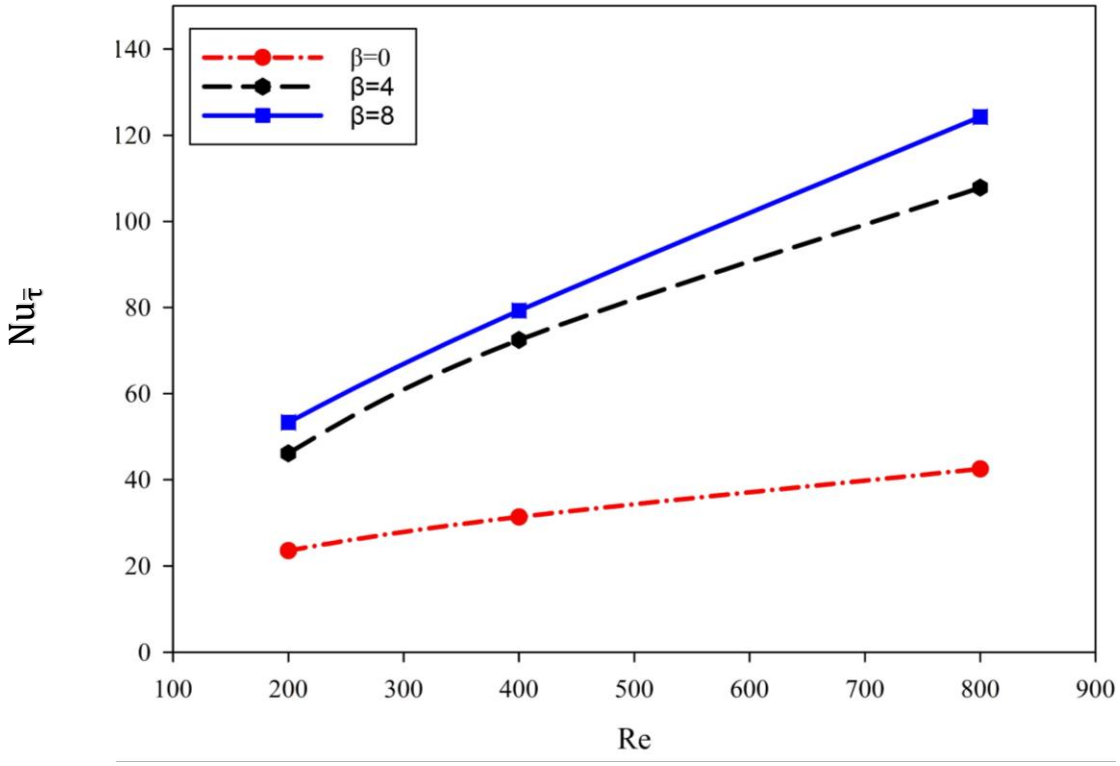

Figure (4- 10) the relation between Time-averaged Nusselt number ($Nu_{\bar{\tau}}$) with Reynolds numbers (Re) at different wavy number (β).

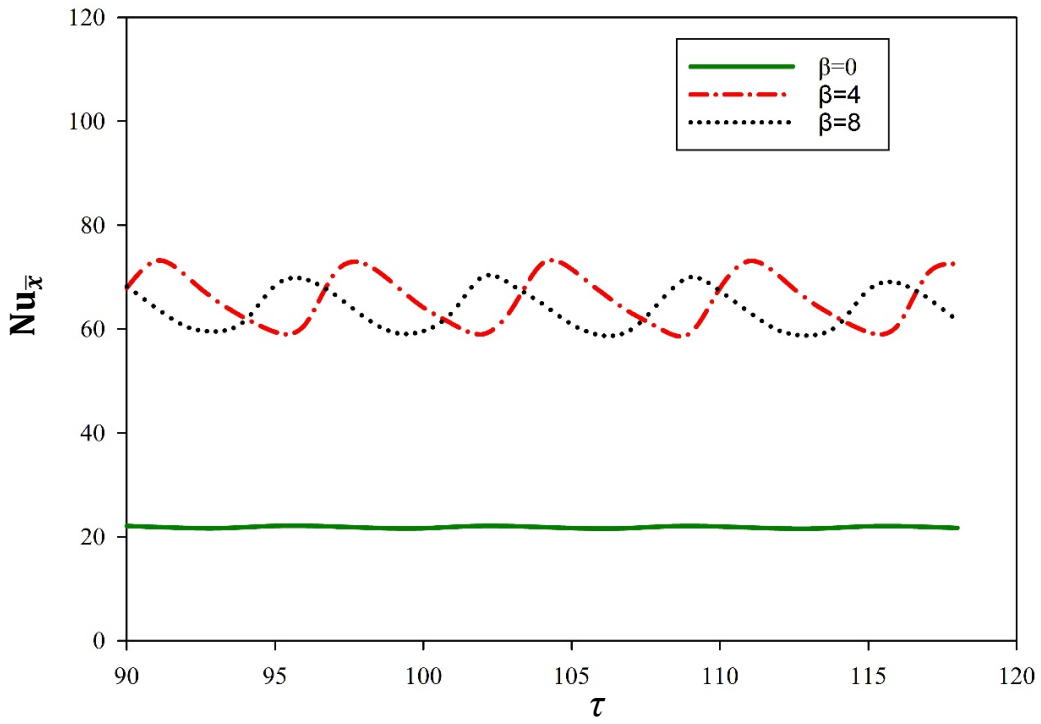

Figure (4- 11) the relation between the variation of space average Nusselt number ($Nu_{\bar{x}}$) with time at different wavy number (β) and Re = 400.

4.3.2.2 Local Nusselt Number

Figures (4-12 to 4-13) show the relationship between local Nusselt number (Nu), arc length (x), and different value of wavy number (β) at St = 0.15, Re=400, Pr=31.4 and α= 0.2. From the figures that explain the relationship between the flow and the number of wavy. It was noticed the flow near to be smooth when the value of (β=0) and the value of (Nu). It is near to be constant (Nu=12.536) for all point, as shown in Figure (4-12), in Figure (4-13) it was noticed the value of (Nu) increases with increasing (β=2) and this increase continues with an increase in the value of (β) where the value of (Nu) between (4.9 and 49.89) and become between (1.5 and 100) at (β=8). Therefore, this increase affects the shape of the flow and enhancement of heat transfer.

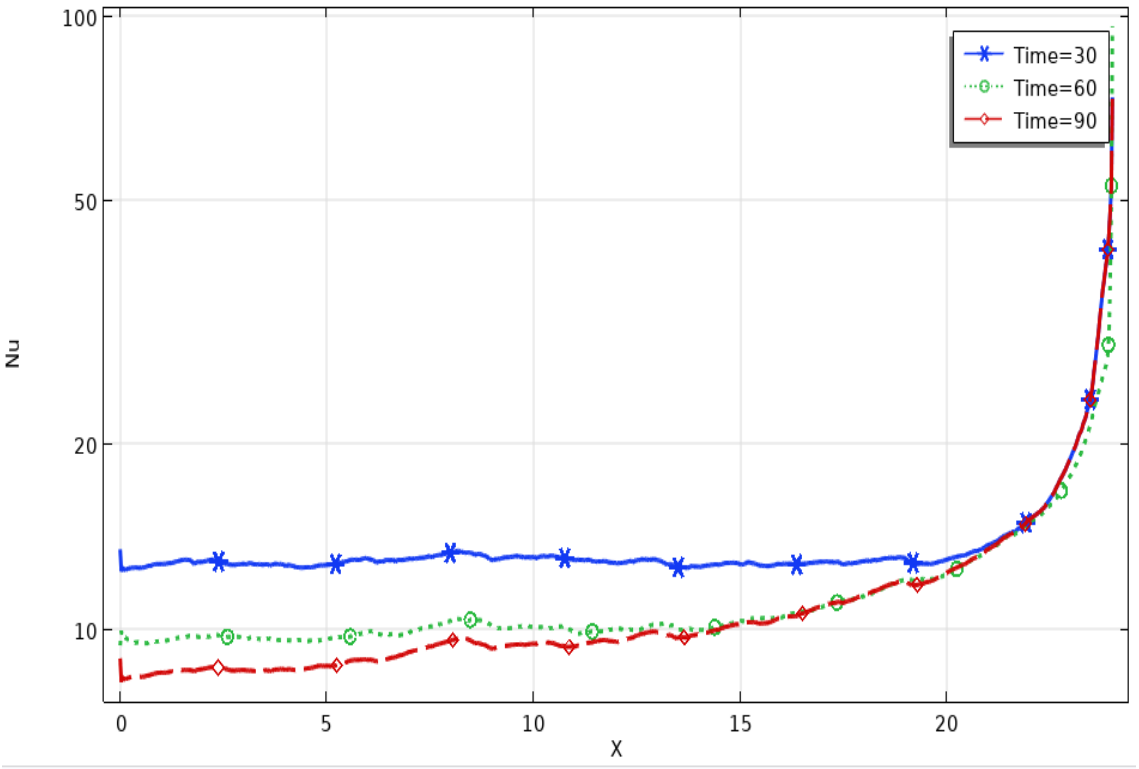

Figure (4- 12) the relation between Nusselt number distribution along the wall channel under pulsing flow with β=0 at different time.

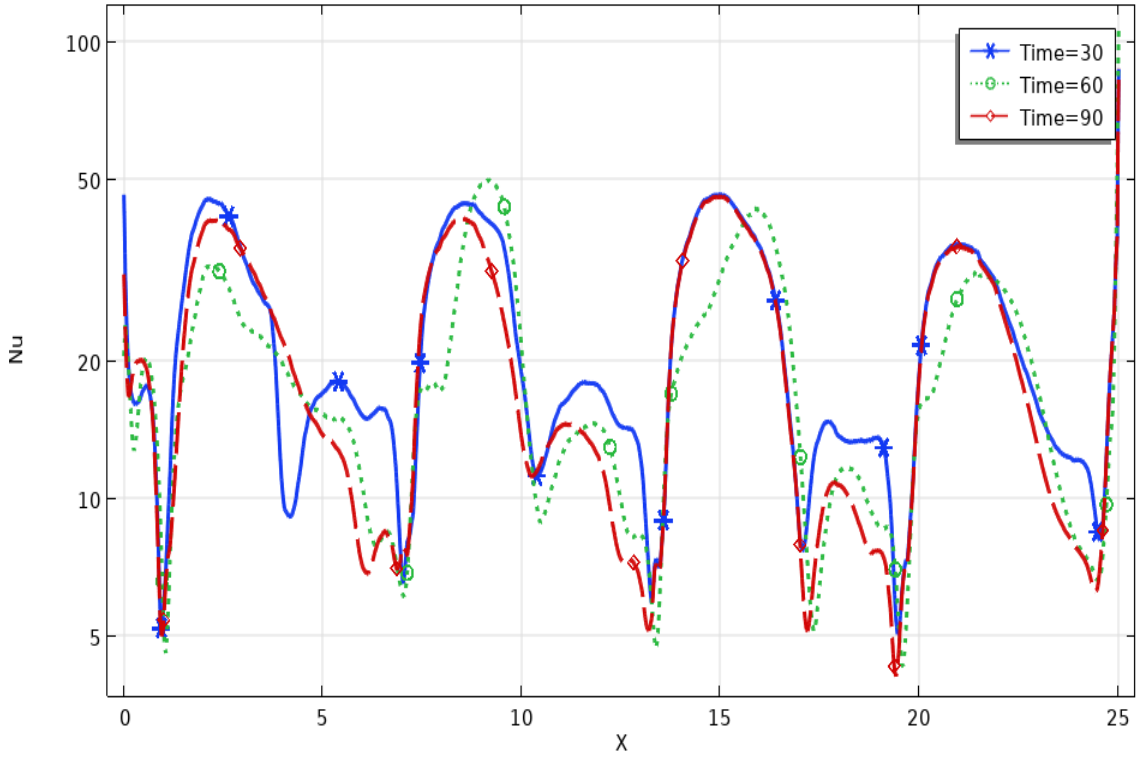

Figure (4- 13) the relation between Nusselt number distribution along the wall channel under pulsing flow with β=2 at different time.

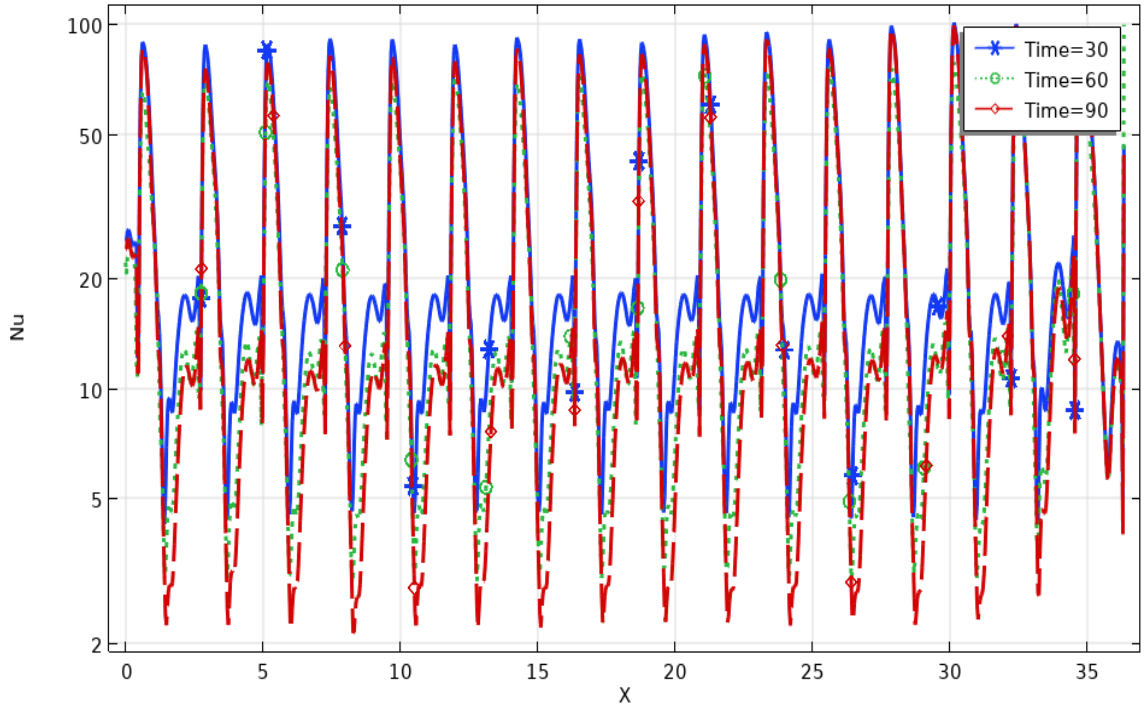

Figure (4- 14) the relation between Nusselt number distribution along the wall channel under pulsing flow with β=8 at different time.

4.3.3 Effect of Amplitude of Wave Channel.

4.3.3.1 Average Nusselt Number space average Nusselt number.

Figures (4- 15 and 4- 17) show the relationship between Time-averaged Nusselt number ($Nu_{\bar{\tau}}$) and wavy amplitude (α) at different Reynolds numbers (Re) when the flow is fully developed with different Reynolds numbers. It is observed that at a very low Reynolds number and low amplitude of pulse the Nu value is almost close to the steady case (Re =200 & α = 0). This is because the surface geometry of the wavy channel has no effect on the main flow and the flow seems to be dominated by viscous forces, the flow in the wavy passages is characterized by the steady flow. However, as the Re is increased beyond a modest value, the pulsating inlet flow at all amplitude ($0 \leq \alpha \leq 0.3$) predominates viscous force which is superimposed with the main flow and the flow becomes unsteady with the rolling up of the shear layer with the channel wall fluid. The unsteady flow improves the mixing process between the core and near-wall fluid resulting in a significant increase in heat transfer compared to the steady case. Through the figure, it was noticed that the amount of ($Nu_{\bar{\tau}}$) increased with the increasing of (α). As well as with the increase of the amount of (Re) where ($Nu_{\bar{\tau}}$=22.1603) at (α=0, Re=200) and it continues increasing where its value become ($Nu_{\bar{\tau}}$=62.7446) at (α=0.3, Re=200) and also increasing for the same value of (α=0) but with increasing Reynolds numbers (Re=800) where the value becomes ($Nu_{\bar{\tau}}$=39.07). As a result, it was noticed that increasing (α) improves heat transfer significantly.

Figure (4-17) shows the relationship between space average Nusselt number ($Nu_{\bar{x}}$), time at different values of wavy amplitude (α), and a constant value of (Re = 400). It was noticed that the value of ($Nu_{\bar{x}}$) is constant with time but increases with increasing value (α). And it was noticed the amount of pulsating flow remains constant with time but increased with increasing the

value of (α) and its value continue increased with increase (α). Through Figure (4- 17) it was noticed that the value of (α=0) the flow is near to be no pulsing.

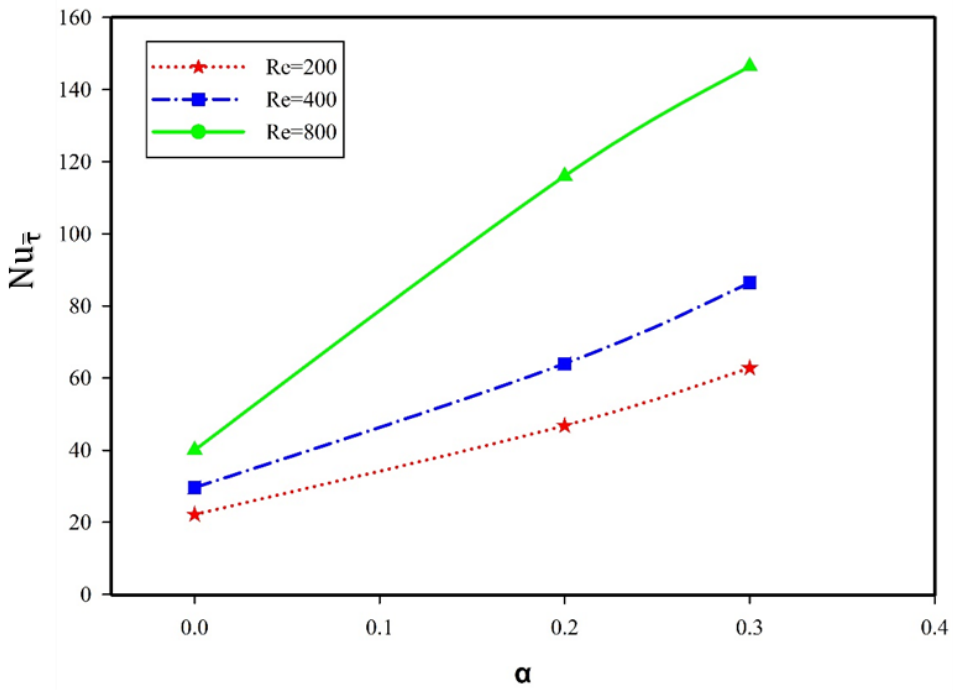

Figure (4- 15) the relation between Time-averaged Nusselt number ($Nu_{\bar{\tau}}$ ***) with wavy amplitude (α) at different Reynolds numbers (Re).***

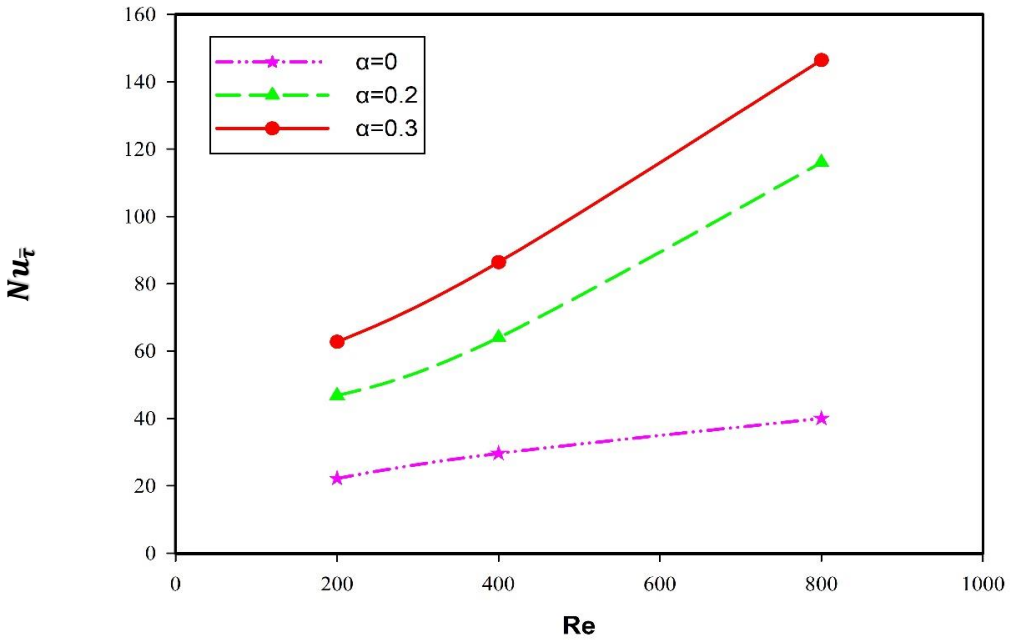

Figure (4- 16) the relation between Time-averaged Nusselt number ($Nu_{\bar{\tau}}$ ***) with Reynolds numbers (Re) at different wavy amplitude (α).***

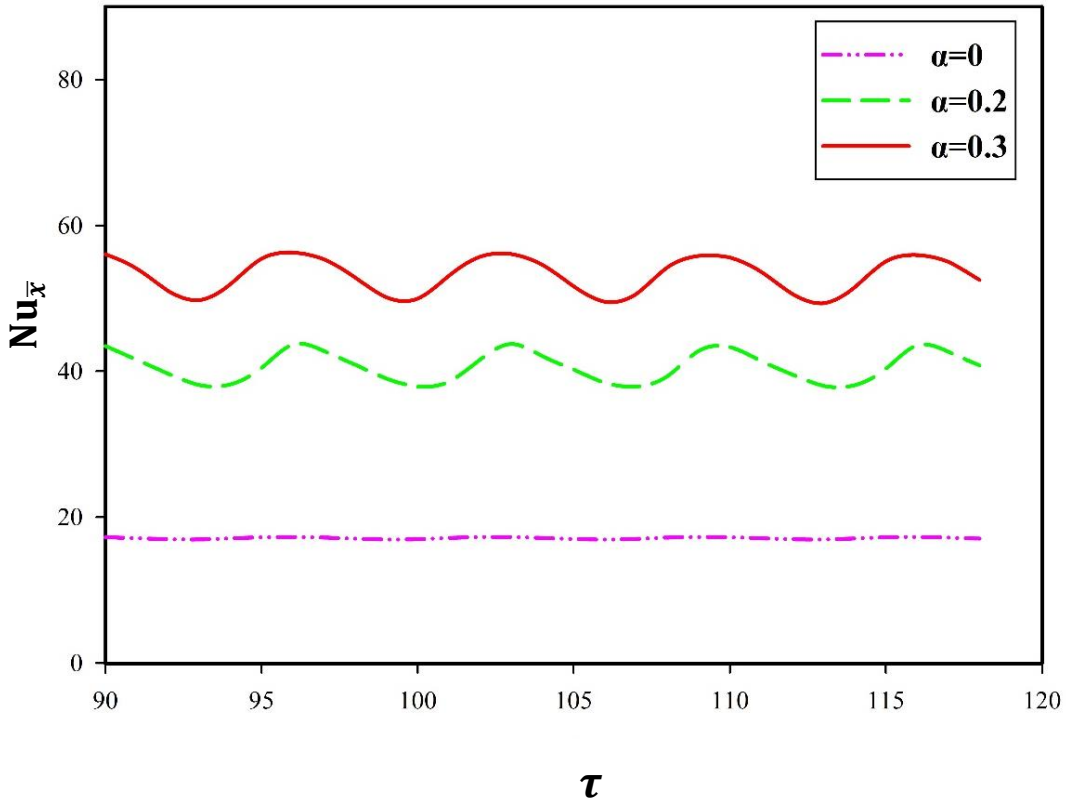

Figure (4- 17) the relation between the variation of space average Nusselt number ($Nu_{\bar{x}}$***) with time at different wavy amplitude (α) and Re = 400.***

4.3.3.2 Local Nusselt Number

Figures (4- 18, 4-19, and 4-20) show the relationship between local Nusselt number (Nu), arc length (x), and different value of wavy amplitude (α) at St = 0.15, Re=400, Pr=31.4, and β= 6. From the figures, explain the relationship between the flow and the wavy amplitude it was noticed that the flow near to be smooth when the value of (α=0) and the value of (Nu) it is near to be constant (Nu=12.536) for all point, as shown in Figure (4-18).in figure (4-20), it was noticed that the value of (Nu) increased with increasing (α=0.2) and this increase continues with increasing in the value of (α) where the value of (Nu) between (5 and 50) and become between(2 and 60) at (α =0.3). Therefore, this increase affects the shape of the flow and enhance of heat transfer.

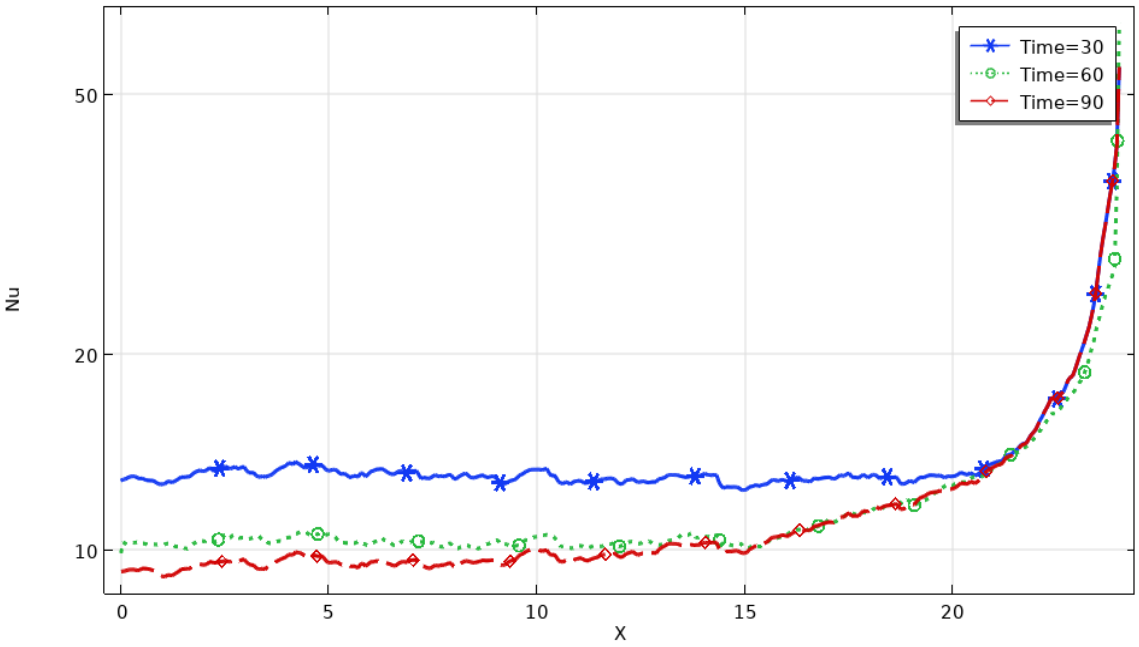

Figure (4- 18) the relation between local Nusselt number distribution along the wall channel under pulsing flow with α= 0 at different time.

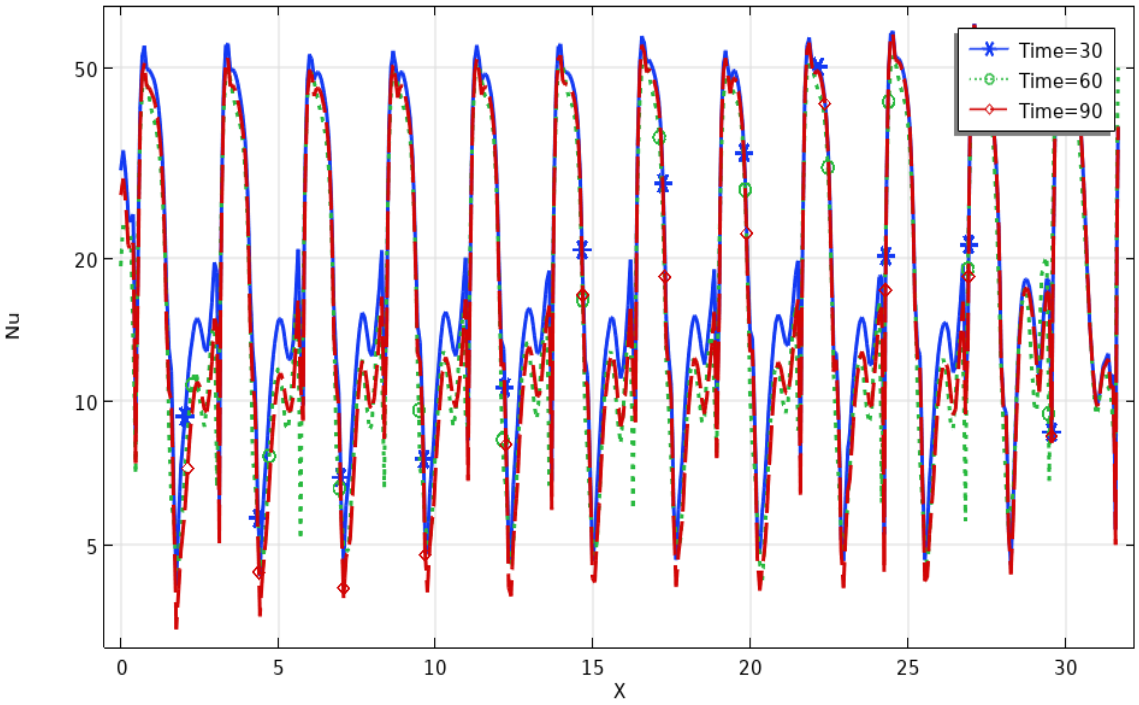

Figure (4- 19) the relation between local Nusselt number distribution along the wall channel under pulsing flow with α= 0.2 at different time.

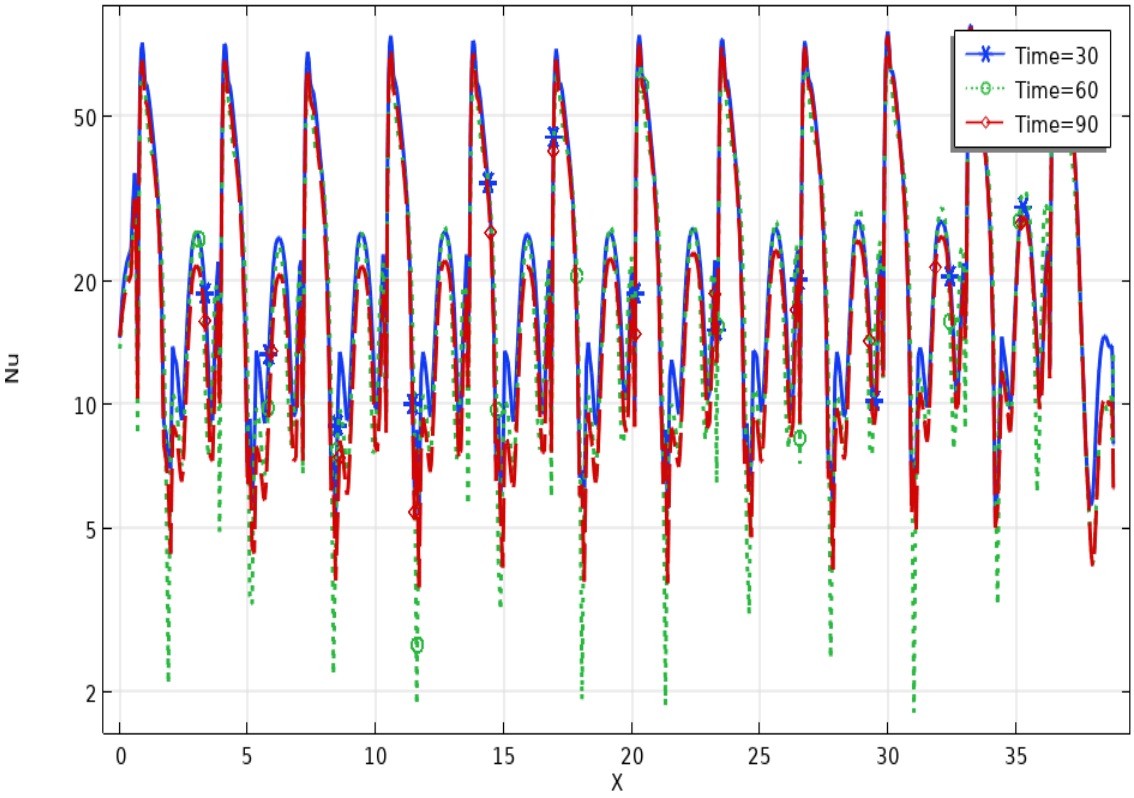

Figure (4- 20) the relation between local Nusselt number distribution along the wall channel under pulsing flow with α= 0.3 at different time.

4.3.4 Streamlines and isothermal Results

4.3.4.1 Streamlines: Effect of Strouhal Numbers.

Figures (4-21 to 4-22) show the streamline contour and isothermal contour for different values of (St) at different times (30,60). Figure (4-21) shows the effect of (St) on streamline at different times (30,60). It was noticed that the streamline at the inlet be smooth and parallel to each other when the time increase with increasing the value of St it noticed the vortex become generated in the flow of channel and it are in the large value near to the wavy wall.

Therefore, the greater the growth of the vortices in the flow, the greater the rate of heat transfer improvement.

Figure (4-22), illustrates the effect of the (St) number on the isothermal, where we notice that increasing the (St) number leads to an increase in the velocity of the flow, and that lead to an increase in the gradient with

temperature, and this can be observed at (St) of 0 with time, the gradient in the isothermal is lower value and become in high value when the value of St becomes 0.15 when the time are 60.

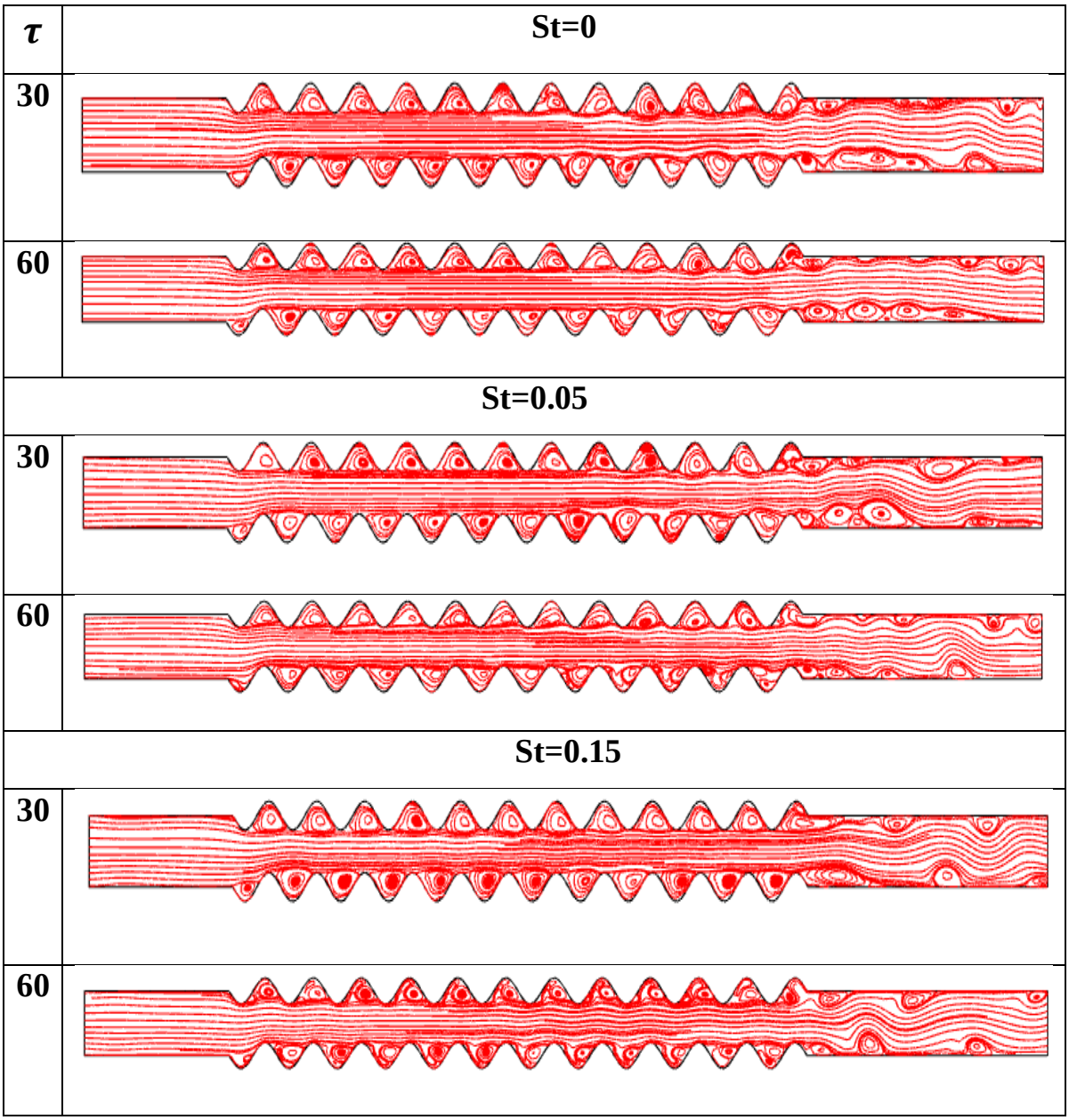

Figure (4- 21) the Streamlines contour for different value of Strouhal Numbers and time.

4.3.4.2 Isothermal: Effect of Strouhal Numbers

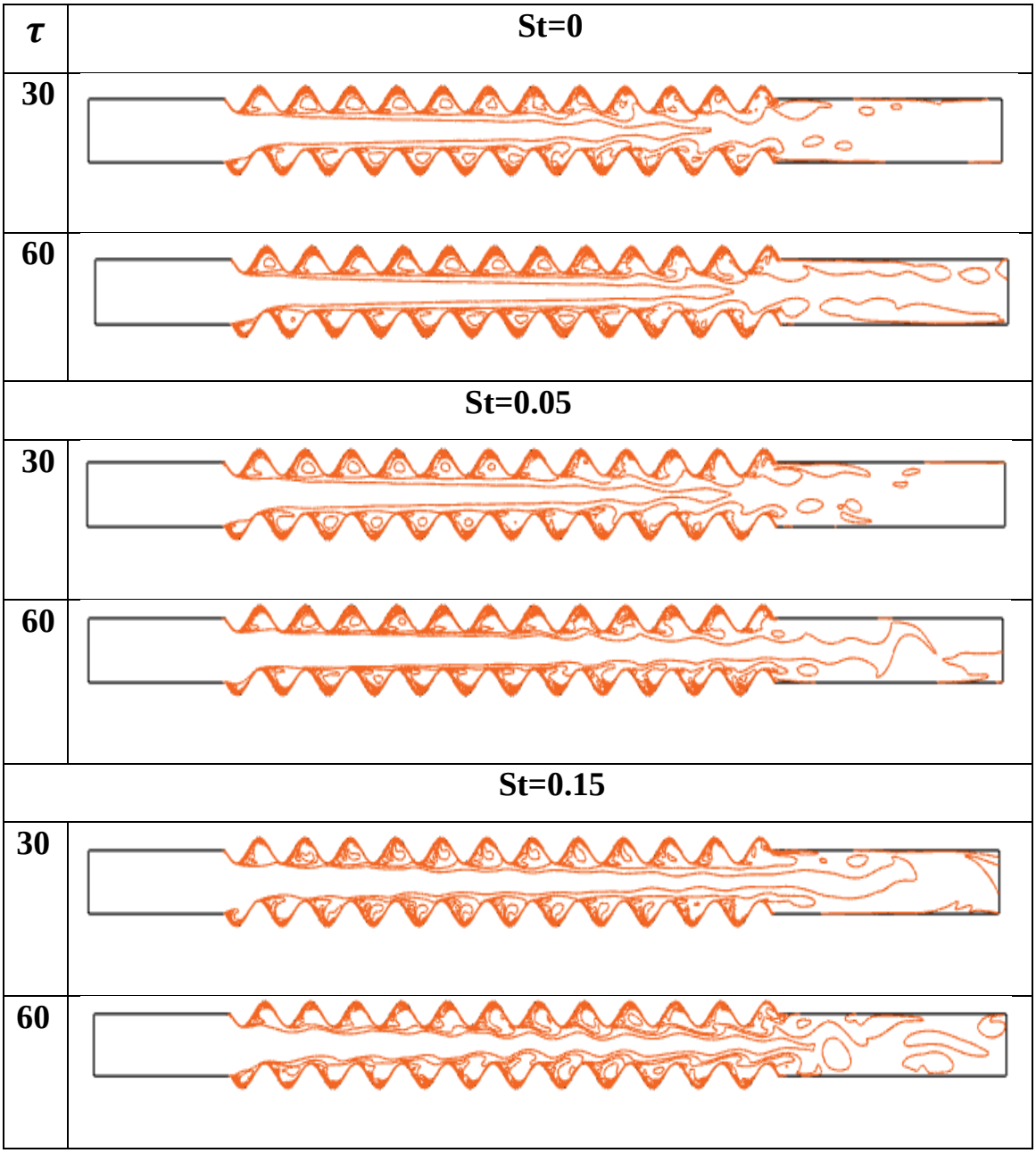

Figure (4- 22) the isothermal contour for different value of Strouhal Numbers and time.

4.3.4.3 Streamlines: Effect of wavy number

Figure (4-23) shows the effect of (β) on streamlining at different times (30,60), as the wavy number effect on the channel shape and this effecting on fluid flow led to enhance the heat transfer in the wavy channel. Whereat (β=0), it was noticed that the flow is smooth and there's no vortex in the

channel, as the value of (β) increase, so this effecting on flow where vortex starts growth in the wavy shape when the number of waves increases so the effect will increase and cause growing more vortexes, so more vortex growth led to enhancement in heat transfer.

Figure (4-24) represents the effect of the number of waves on the isothermal. This effect can be observed with the increase in the number of waves, where noticed the gradient in temperature when the value of (β=0) in a lower value for all time and it seen near the wall, but when the value of (β) increase it noticed the gradient in temperature in the core, and it increases with increasing the value of time this means an improvement in heat transfer.

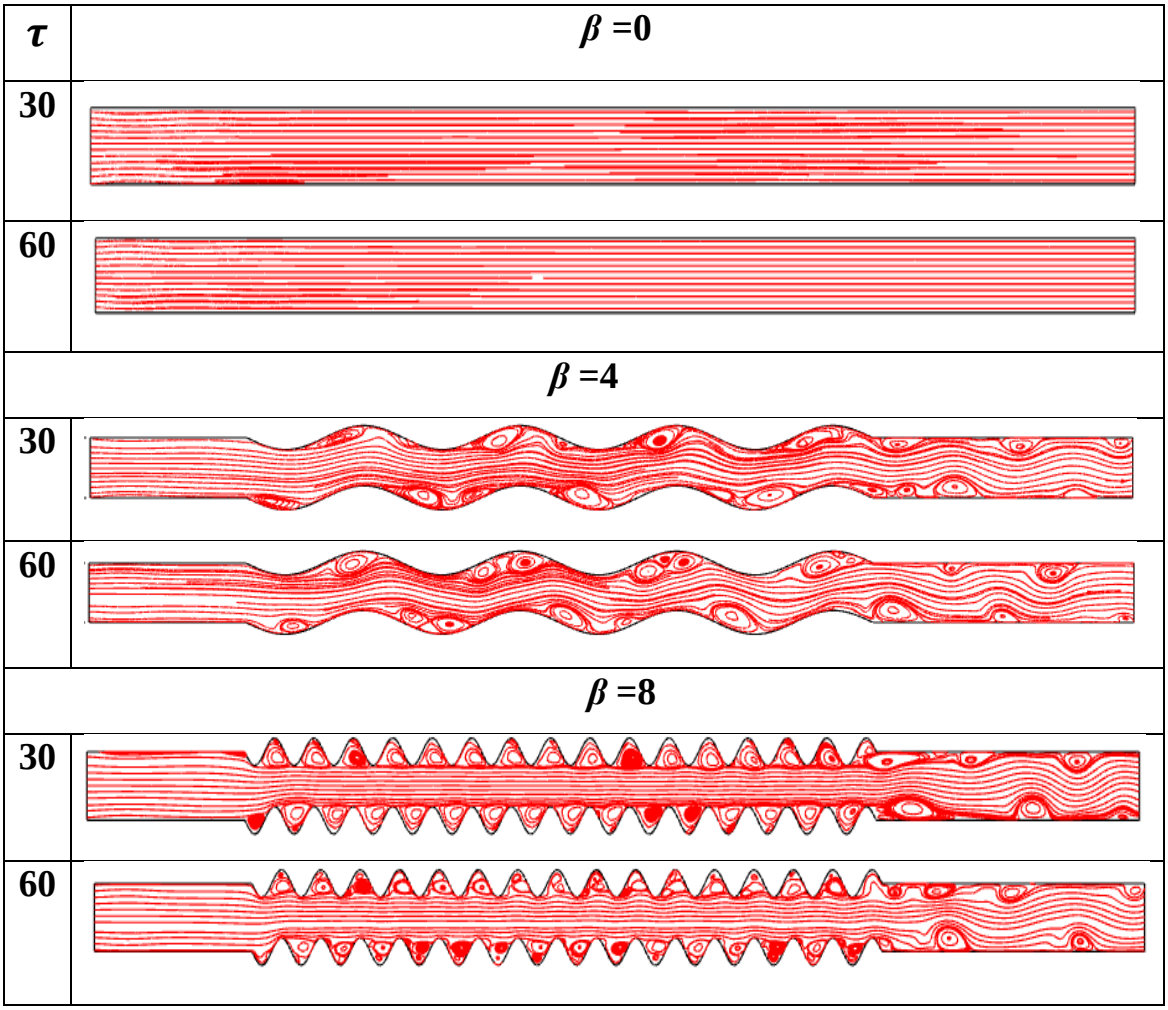

Figure (4- 23) the streamline contour for different value of wavy number and time.

4.3.4.4 Isothermal: Effect of wavy number.

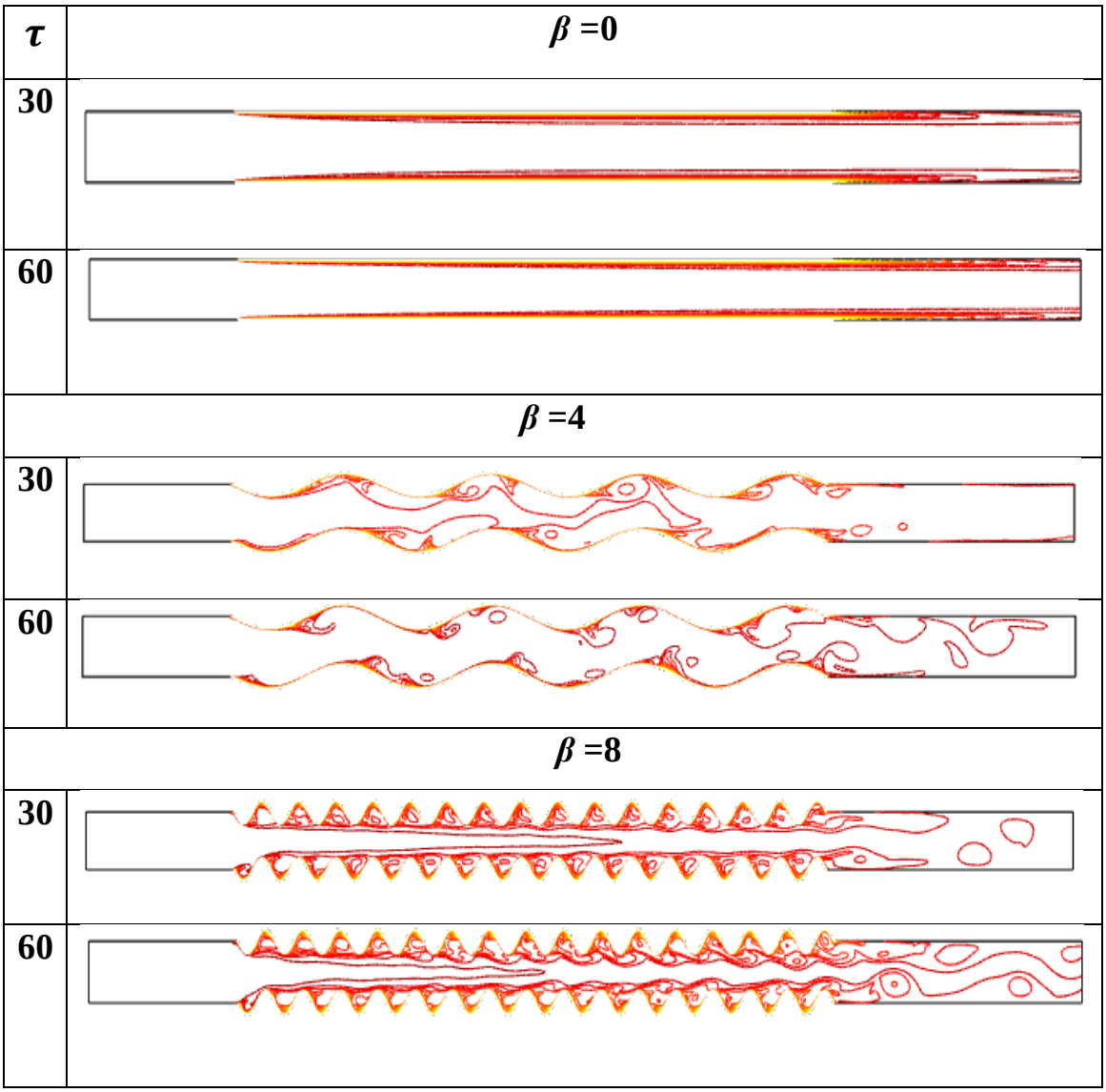

Figure (4-24) the isothermal contour for different value of wavy number and time.

4.3.4.5 Streamlines: Effect of Wavy Amplitude.

Figure (4-25) shows the effect of(α) on streamlining at different times (30,60), as the wavy amplitude effect on the channel shape and this effecting on fluid flow and enhancement of heat transfer in this wavy channel, from the figure it noticed that the flow is to be smooth at (α=0) and this means no vortex grow in the channel, when the value of the wavy amplitude increase, it will affect the flow where the vortex starts growth in the wavy shape and

when (α=0.3) it noticed how vortexes became, how it grew faster and become in max value.

Figure (4-26) represents the effect of the wavy amplitude on the isothermal. This effect can be observed with the increase in the wavy amplitude, where noticed the gradient in temperature when the value of (α =0) in a lower value for all time and it seen near the wall, but when the value of (α) increase it is noticed the gradient in temperature in the core, and it increases with increasing the value of time, and when the value of (α =0.3) the gradient in temperature it be higher value with time this means an improvement in heat transfer.

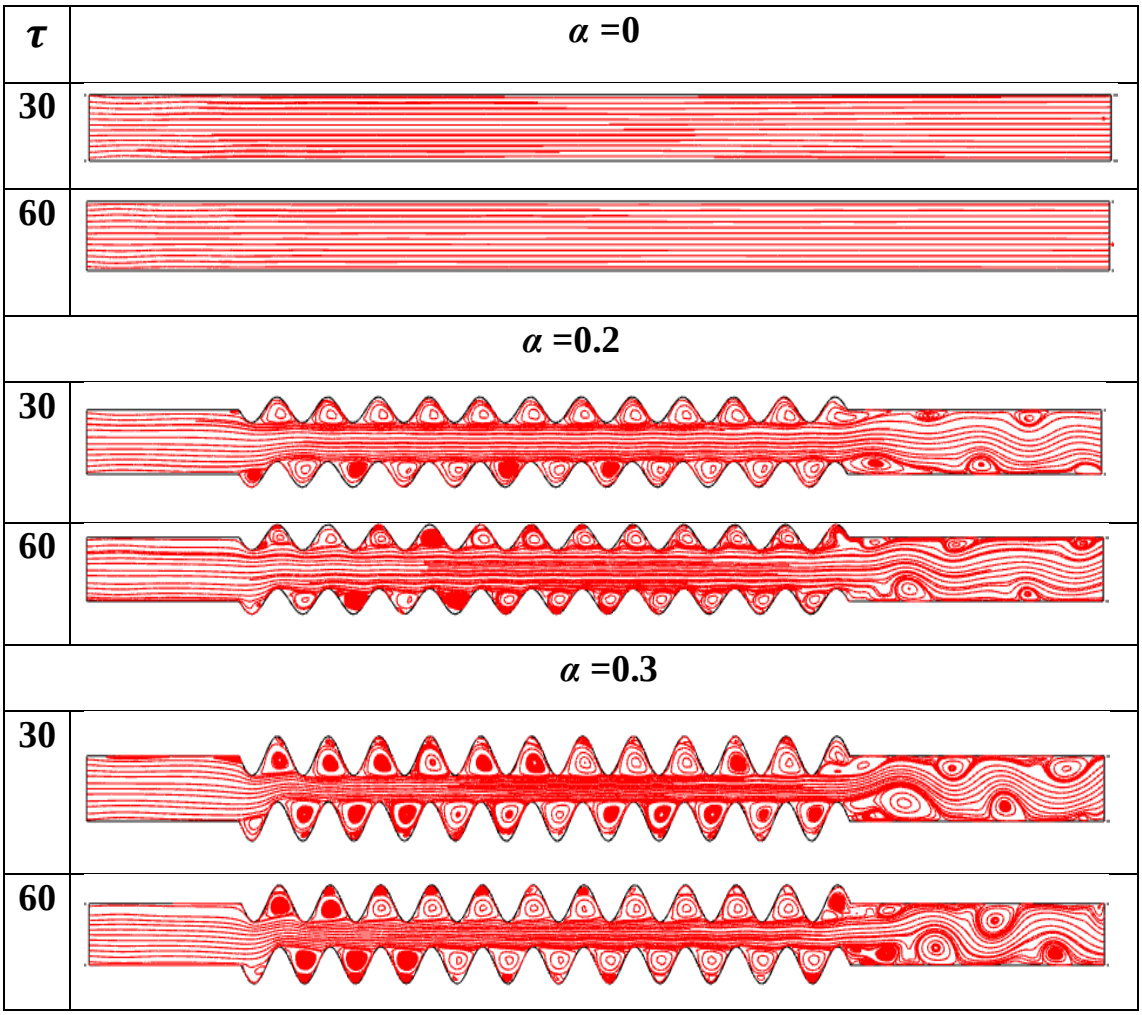

Figure (4-25) the isothermal contour for different value of amplitude of wave channel and time.

4.3.4.6 Isothermal: Effect of Wavy Amplitude.

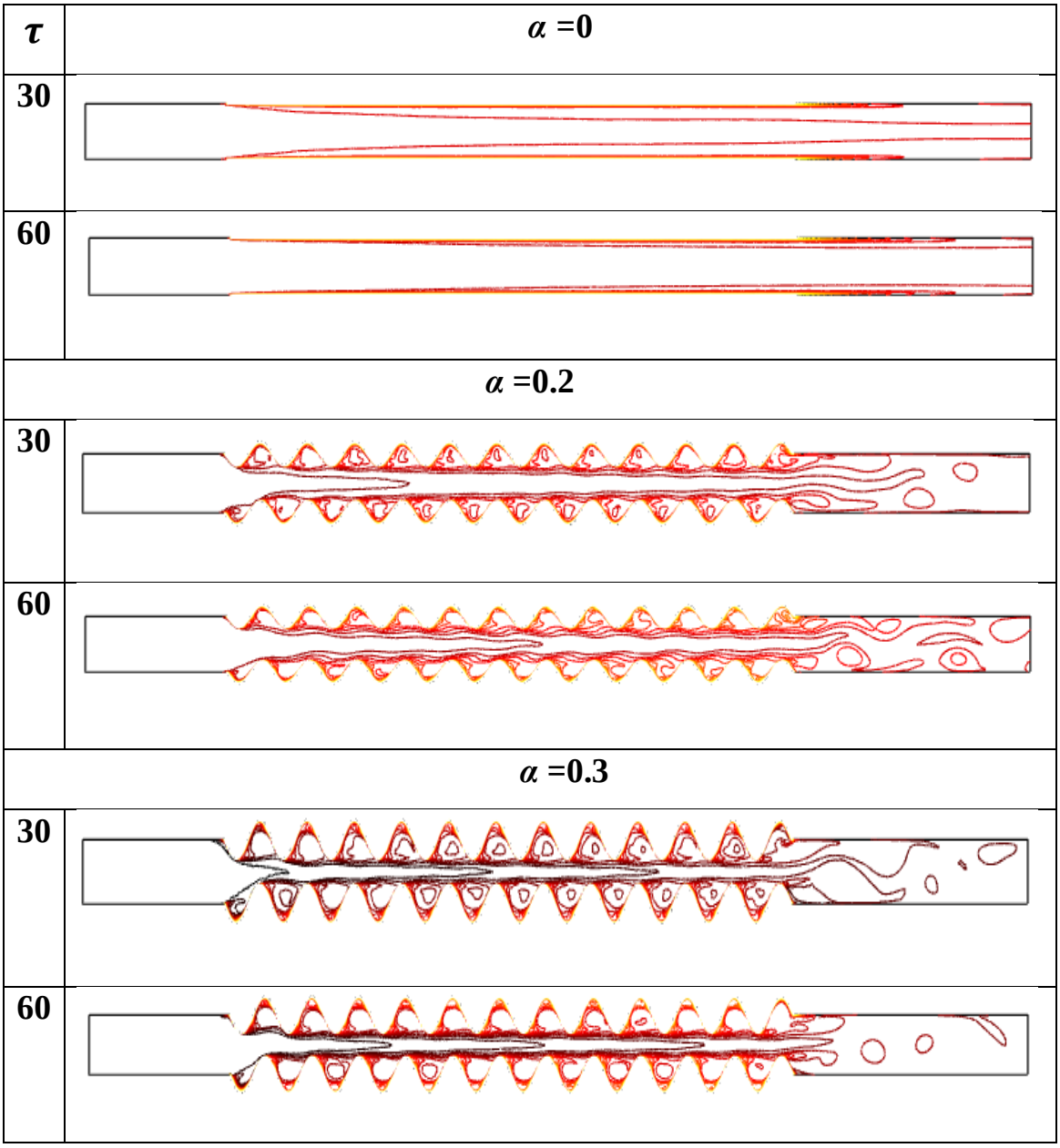

Figure (4-26) the isothermal contour for different value of amplitude of wave channel and time.

Through the Table (4-1), it can be noticed that the percentages of improvement in the value of Nusselt number when increasing the number of waves through the channel. So, the increase in the number of waves leads to an increase in the surface area of heat transfer as well as leads to the

generation of vortices that contribute to As the heat transfer coefficient rises, the number of Nusselt rises as well where it noted that the percentage of improvement also increased by (1.439) at the Reynolds number 200, when using the number of 10 waves, while it reached the highest value at the Reynolds number 800 and the number of 8 waves, where the value of the Nusselt number was equal to (1.923306).

With the same behavior, Table (4-2) represents the percentages indicating the improvement in the value of the Nusselt number, depending on the value of the wave Amplitude. The higher Amplitude, the greater the value of the Nusselt Number. To reach its highest value at Amplitude (0.3) which is equal to 2.663 at the Reynolds number 800.

With the same behavior, Table (4-3) represents the percentages indicating the improvement in the value of the Nusselt number, depending on the value of the Strouhal number. The higher Strouhal number, the greater the value of the Nusselt Number. To reach its highest value at Strouhal number (0.15) which is equal to 0.133 at the Reynolds number 800.

Table (4- 1) The percentage of improvement in the value of the Nusselt number when changing wave number.

Re	Time-averaged Nusselt number				
	β=0	β=4	Enhancement	β=8	Enhancement
200	23.56	46.14	0.957	53.31	1.262
400	31.38	72.44	1.308	79.22	1.524
800	42.50785	107.8263	1.53662	124.2634	1.923306

Table (4- 2) The percentage of improvement in the value of the Nusselt number when changing wave amplitude.

Re	Time-averaged Nusselt number				
	α=0	α=0.2	Enhancement	α=0.3	Enhancement
200	22.16	46.78	1.1113	62.744	1.831
400	29.59	63.96	1.1612	86.392	1.919
800	39.97	116.05	1.9029	146.45	2.663

Table (4- 3) The percentage of improvement in the value of the Nusselt number when changing Strouhal number.

Re	Time-averaged Nusselt number				
	St=0	St=0.05	Enhancement	St=0.15	Enhancement
200	46.34	46.52	0.003	49.66	0.071
400	66.45	67.13	0.010	75.93	0.142
800	102.40	105.89	0.034	116.05	0.133

Chapter Five

Conclusions and Suggestions for Future Work

Chapter Five: Conclusions and Suggestions for Future Work

5.1 Conclusions

The numerical study was carried out on a wavy channel with a sinusoidal function and a pulsing flow. The dimensions of the channel were changed, which included the change in the number of waves as well as the wave height. Different value of Reynolds number and Strouhal number, were used to show the effect of pulsing flow of kerosene fuel, the following points can be concluded:

1- Increasing the number of waves leads to increase in the value of the Nusselt number. Compared to the flat channel, the percentage of improvement with the value of the Nusselt number reached 1.262 at the value of Reynolds number 200, while it reached 1.923306 at the Reynolds number 800, and $\beta=8$ wave number. Therefore, the increasing in the Reynolds number leads to an increase in the improvement in heat transfer.

2- Through the numerical analysis, it was observed that the improvement percentage increased by the value of the Nusselt number when increasing the amplitude of the wave, the percentage of improvement with the value of the Nusselt number reached 0.756 at the value of Reynolds number 200 and $\alpha=0$, while it reached 2.663 at the Reynolds number 800, and $\alpha=0.3$, Therefore, the increasing the surface area leads to increase the value of Nusselt Number and caused to improve a heat transfer.

3- The use of pulsing flow effectively enhanced the process of heat transfer compared to a steady flow, Heat transfer enhancement is not significant and the effect of the Reynolds number is limited for the Strouhal number of St=0.05, So a percentage of improvement with the

value of the Nusselt number reached 0.003 at Reynolds number 200 and St=0.05 and increased to 0.264 at the value of Reynolds number 800 and St=0.15, So it was noted that the effect of the value of the Strouhal number on the improvement of heat transfer, as the more it increases, the value of the Nusselt number will increase.

5.2 Suggestions for Future Work

The following suggestions could be made based on this research for potential projects:

1- Study the effect of using hybrid nano fuel with the same channel shape proposed in this study.

2- Study of turbulent flow for the same types of fuel used in this study.

3- Investigate the effect of adding an intermediate layer of phase changed materials (PCM).

REFRENCES

References

[1] Kadim, Zena Khalefa, and Kamil Abdulhussein Khalaf. "Numerical Study of Heat Transfer Enhancement in Contour Corrugated Channel Using Water and Engine Oil." *CFD Letters* 12.12 (2020): 17-37.

[2] J. Galindo, P. Fajardo, R. Navarro, and L. M. García-Cuevas, "Characterization of a radial turbocharger turbine in pulsating flow by means of CFD and its application to engine modeling," *Applied Energy*, vol. 103, pp. 116–127, 2013, doi: 10.1016/j.apenergy.2012.09.013.

[3] S. Marelli and M. Capobianco, "Steady and pulsating flow efficiency of a waste-gated turbocharger radial flow turbine for automotive application," *Energy*, vol. 36, no. 1, pp. 459–465, 2011, doi: 10.1016/j.energy.2010.10.019.

[4] B. H. Yan, "Analysis of laminar to turbulent transition of pulsating flow in ocean environment with energy gradient method," *Annals of Nuclear Energy*, vol. 38, no. 12, pp. 2779–2786, Dec. 2011, doi: 10.1016/j.anucene.2011.08.016.

[5] D. Xu, T. Chen, and Y. Xuan, "Thermo-hydrodynamics analysis of vapor-liquid two-phase flow in the flat-plate pulsating heat pipe," *International Communications in Heat and Mass Transfer*, vol. 39, no. 4, pp. 504–508, Apr. 2012, doi: 10.1016/j.icheatmasstransfer.2012.02.002.

[6] W. Chang, G. Pu-Zhen, T. Si-Chao, and X. Chao, "Theoretical analysis of phase-lag in low frequency laminar pulsating flow," *Progress in*

Nuclear Energy, vol. 58, pp. 45–51, Jul. 2012, doi: 10.1016/j.pnucene.2012.02.004.

[7] BEHERA, Alok Narayan. *Heat Transfer in Pulsatile Flow Through Square Microchannels with Wavy Walls*. 2015. PhD Thesis.

[8] T. K. Nandi and H. Chattopadhyay, "Numerical investigations of simultaneously developing flow in wavy microchannels under pulsating inlet flow condition," *International Communications in Heat and Mass Transfer*, vol. 47, pp. 27–31, Oct. 2013, doi: 10.1016/j.icheatmasstransfer.2013.06.008.

[9] H. Zhang, S. Li, J. Cheng, Z. Zheng, X. Li, and F. Li, "Numerical study on the pulsating effect on heat transfer performance of pseudo-plastic fluid flow in a manifold microchannel heat sink," *Applied Thermal Engineering*, vol. 129, pp. 1092–1105, Jan. 2018, doi: 10.1016/j.applthermaleng.2017.10.124.

[10] X. Zhu, J. C. Lisanti, T. F. Guiberti, and W. L. Roberts, "A preliminary investigation of the secondary flame and operational properties of an actively-valved pulse jet," in *AIAA Scitech 2020 Forum*, 2020, vol. 1 PartF. doi: 10.2514/6.2020-0922.

[11] Esfe, Mohammad Hemmat, et al. "A critical review on pulsating flow in conventional fluids and nanofluids: Thermo-hydraulic characteristics." International Communications in Heat and Mass Transfer 120 (2021): 104859.

[12] K. Braga, A. Bejan, and S. Lorent, "Heat Transfer Handbook."

[13] S. W. Chang, A. W. Lees, T. M. Liou, and G. F. Hong, "Heat transfer of a radially rotating furrowed channel with two opposite skewed

sinusoidal wavy walls," *International Journal of Thermal Sciences*, vol. 49, no. 5, pp. 769–785, May 2010, doi: 10.1016/j.ijthermalsci.2009.11.011.

[14] H. Heidary and M. J. Kermani, "Enhancement of heat exchange in a wavy channel linked to a porous domain; a possible duct geometry for fuel cells," *International Communications in Heat and Mass Transfer*, vol. 39, no. 1, pp. 112–120, Jan. 2012, doi: 10.1016/j.icheatmasstransfer.2011.10.001.

[15] S. Harikrishnan and S. Tiwari, "Heat transfer characteristics of sinusoidal wavy channel with secondary corrugations," *International Journal of Thermal Sciences*, vol. 145, Nov. 2019, doi: 10.1016/j.ijthermalsci.2019.105973.

[16] Akdag, Unal, Selma Akcay, and Dogan Demiral. "Heat transfer enhancement with nanofluids under laminar pulsating flow in a trapezoidal-corrugated channel." *Progress in Computational Fluid Dynamics, An International Journal* 17.5 (2017): 302-312.

[17] Honnet, S., Seshadri, K., Niemann, U., & Peters, N. (2009). A surrogate fuel for kerosene. *Proceedings of the Combustion Institute*, *32*(1), 485-492.

[18] M. Jafari, M. Farhadi, and K. Sedighi, "Pulsating flow effects on convection heat transfer in a corrugated channel: A LBM approach," *International Communications in Heat and Mass Transfer*, vol. 45, pp. 146–154, Jul. 2013, doi: 10.1016/j.icheatmasstransfer.2013.04.006.

[19] Zontul, Harun, Nazım Kurtulmuş, and Beşir Şahin. "Pulsating flow and heat transfer in wavy channel with zero-degree phase shift." *European Mechanical Science* 1.1 (2017): 31-38.

[20] B. Yang, T. Gao, J. Gong, and J. Li, “Numerical investigation on flow and heat transfer of pulsating flow in various ribbed channels,” *Applied Thermal Engineering*, vol. 145, pp. 576–589, Dec. 2018, doi: 10.1016/j.applthermaleng.2018.09.041.

[21] H. H. Afrouzi, M. Ahmadian, A. Moshfegh, D. Toghraie, and A. Javadzadegan, “Statistical analysis of pulsating non-Newtonian flow in a corrugated channel using Lattice-Boltzmann method,” *Physica A: Statistical Mechanics and its Applications*, vol. 535, Dec. 2019, doi: 10.1016/j.physa.2019.122486.

[22] N. Kurtulmuş and B. Sahin, “Experimental investigation of pulsating flow structures and heat transfer characteristics in sinusoidal channels,” *International Journal of Mechanical Sciences*, vol. 167, Feb. 2020, doi: 10.1016/j.ijmecsci.2019.105268.

[23] L. Yu, Y. Bian, Y. Liu, and X. Xu, “Experimental analysis on fluid flow and mass transfer characteristics of CMC solutions in wavy-walled tubes for steady and pulsating flow by PIV,” *Applied Thermal Engineering*, vol. 171, May 2020, doi: 10.1016/j.applthermaleng.2020.115098.

[24] I. A. Davletshin, A. N. Mikheev, N. I. Mikheev, and R. R. Shakirov, “Heat transfer and structure of pulsating flow behind a rib,” *International Journal of Heat and Mass Transfer*, vol. 160, Oct. 2020, doi: 10.1016/j.ijheatmasstransfer.2020.120173.

[25] M. Jafari, M. Farhadi, and K. Sedighi, “Convection heat transfer of SWCNT-nanofluid in a corrugated channel under pulsating velocity profile,” *International Communications in Heat and Mass Transfer*,

vol. 67, pp. 137–146, Oct. 2015, doi: 10.1016/j.icheatmasstransfer.2015.07.008.

[26] X. W. Zhu, Y. H. Fu, and J. Q. Zhao, “A novel wavy-tape insert configuration for pipe heat transfer augmentation,” *Energy Conversion and Management*, vol. 127, pp. 140–148, Nov. 2016, doi: 10.1016/j.enconman.2016.09.006.

[27] A. G. Ramgadia and A. K. Saha, “Numerical study of fully developed unsteady flow and heat transfer in asymmetric wavy channels,” *International Journal of Heat and Mass Transfer*, vol. 102, pp. 98–112, Nov. 2016, doi: 10.1016/j.ijheatmasstransfer.2016.05.131.

[28] D. Yuan, W. Zhou, T. Fu, and C. Liu, “Experimental and numerical investigation of heat and mass transfer in non-uniform wavy microchannels,” *International Journal of Thermal Sciences*, vol. 152, Jun. 2020, doi: 10.1016/j.ijthermalsci.2020.106320.

[29] Liu, Zhaohui, et al. "Heat transfer characteristics during subcooled flow boiling of a kerosene kind hydrocarbon fuel in a 1 mm diameter channel." *International Journal of Heat and Mass Transfer* 55.19-20 (2012): 4987-4995.

[30] A. J. Chamkha and F. Selimefendigil, “Forced convection of pulsating nanofluid flow over a backward facing step with various particle shapes,” *Energies*, vol. 11, no. 11, Nov. 2018, doi: 10.3390/en11113068.

Appendix (A): Solution Procedure

1-open model wizard.

Figure (A- 1) select wizard.

2- Select 2-D.

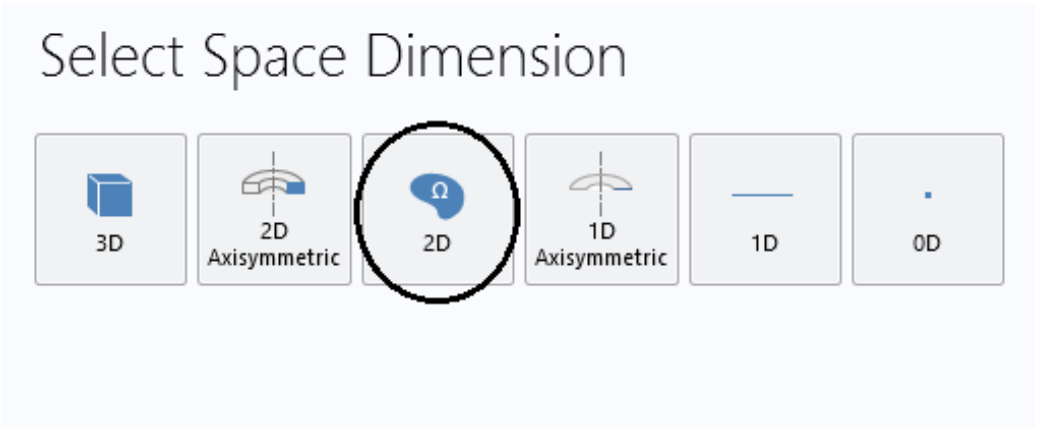

Figure (A- 2) select 2-D.

3- Select physics (Laminar flow) and press add and select (heat transfer) and press add then select (study).

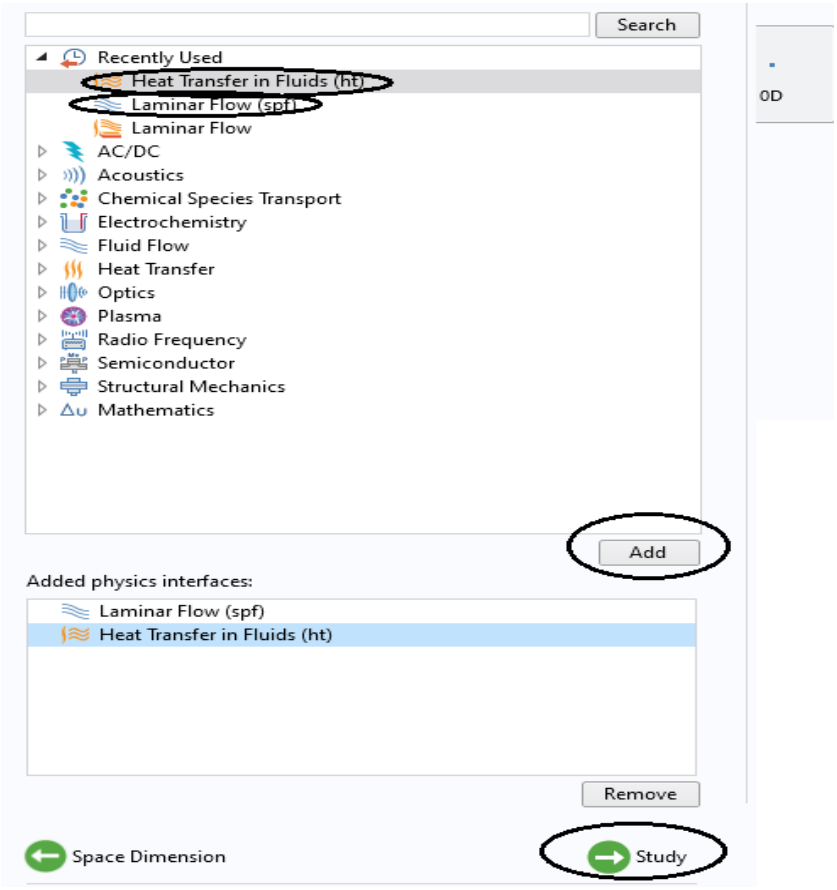

Figure (A- 3) Select physics.

4-general studies: select time dependent and then Done.

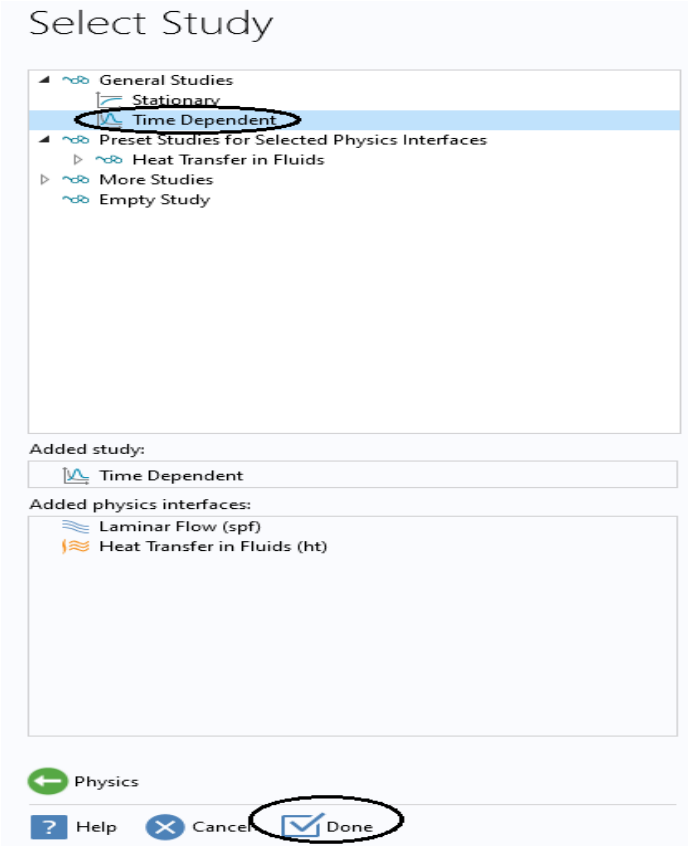

Figure (A- 4) select time dependent.

5-insert the parameters of the study.

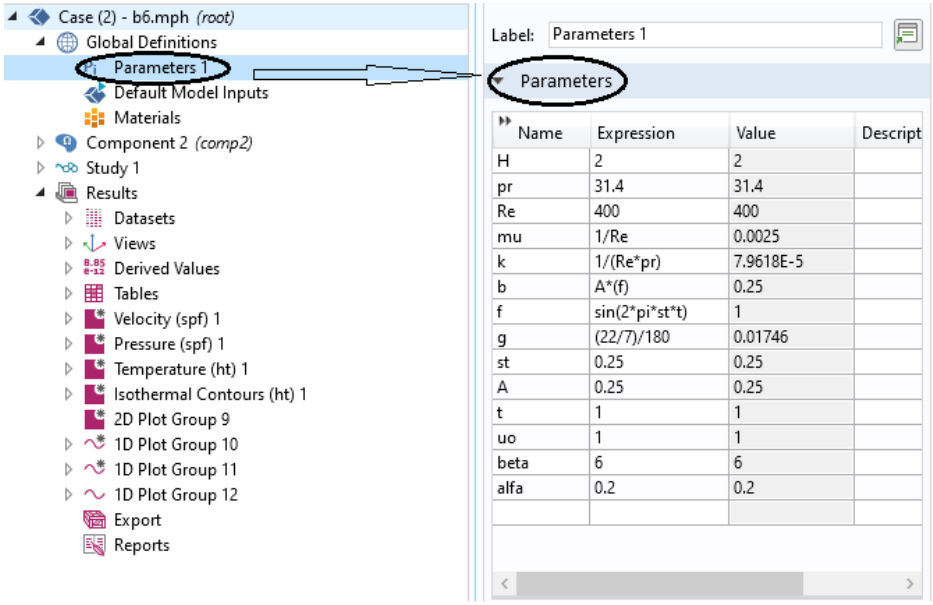

Figure (A- 5) the parameters of the study.

6- Choose the material type of fluid flow and choose.

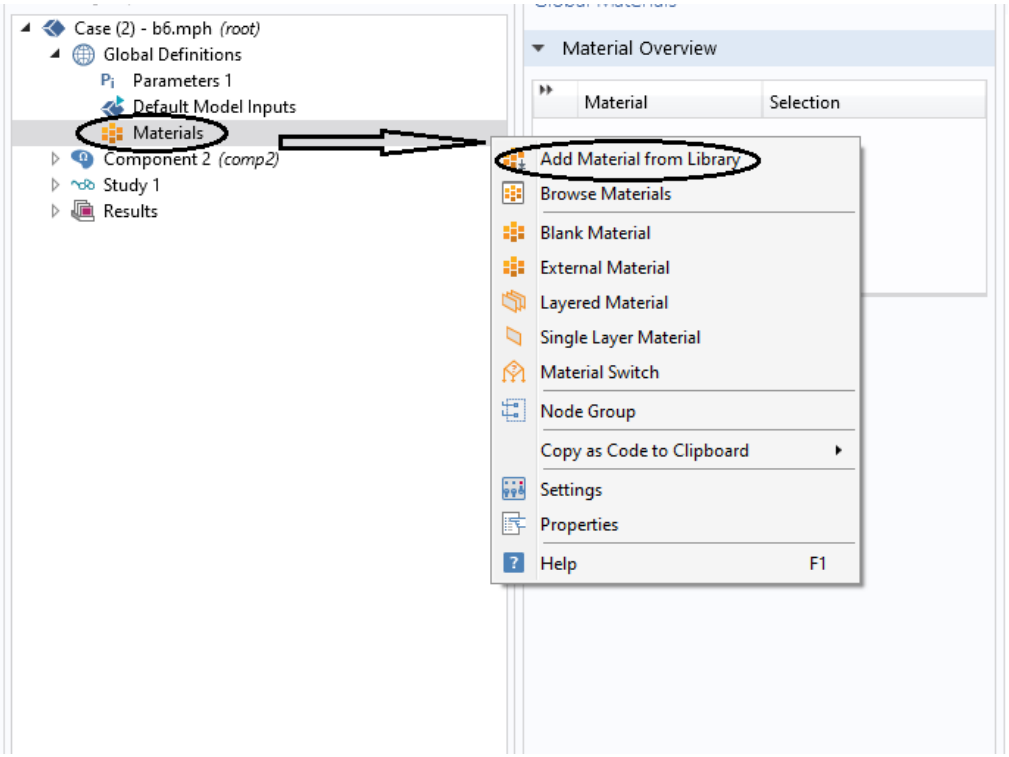

Figure (A- 6) material type of fluid flow.

7-Draw the geometry of wavy channel.

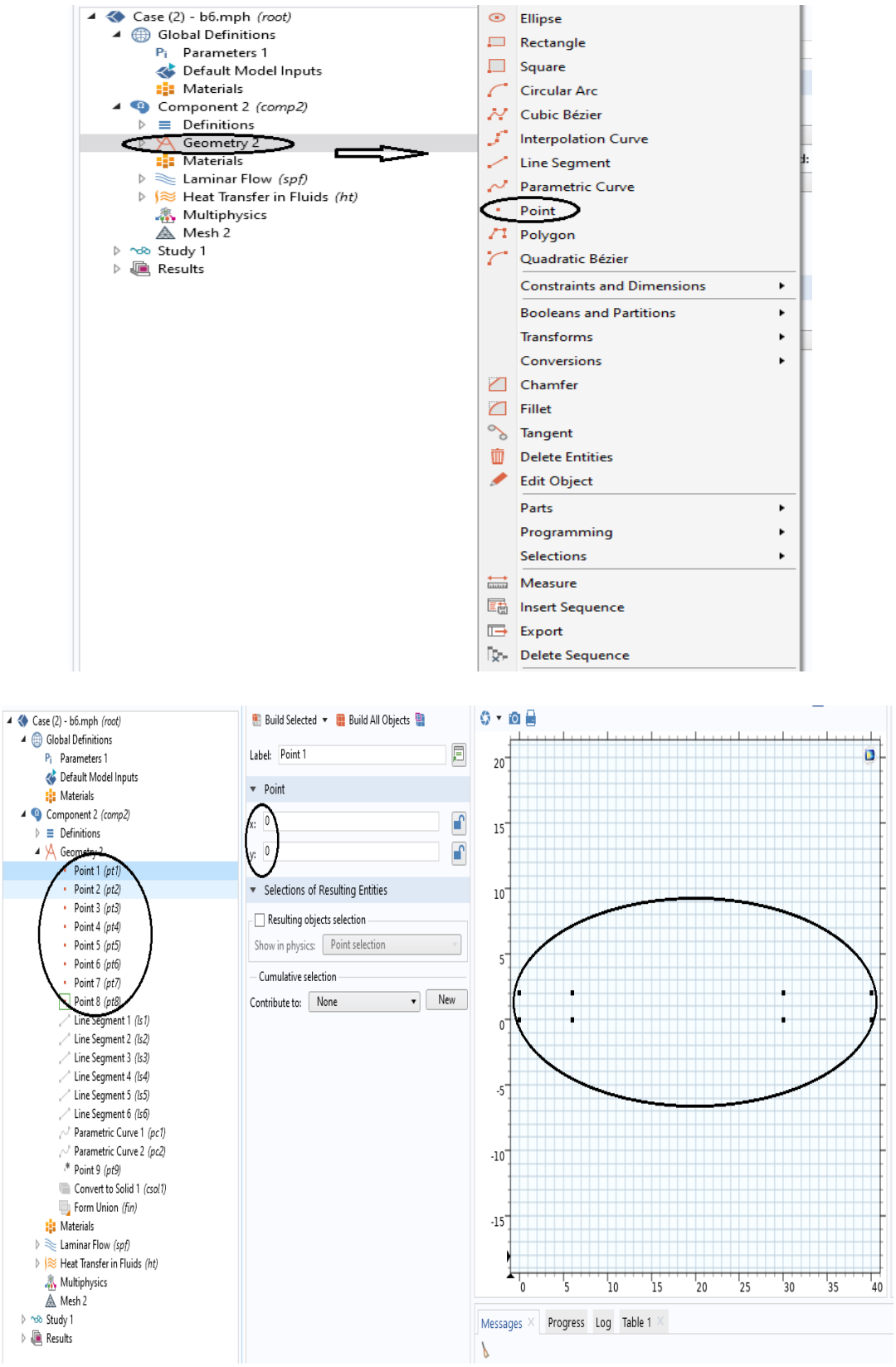

Figure (A- 7) draw point.

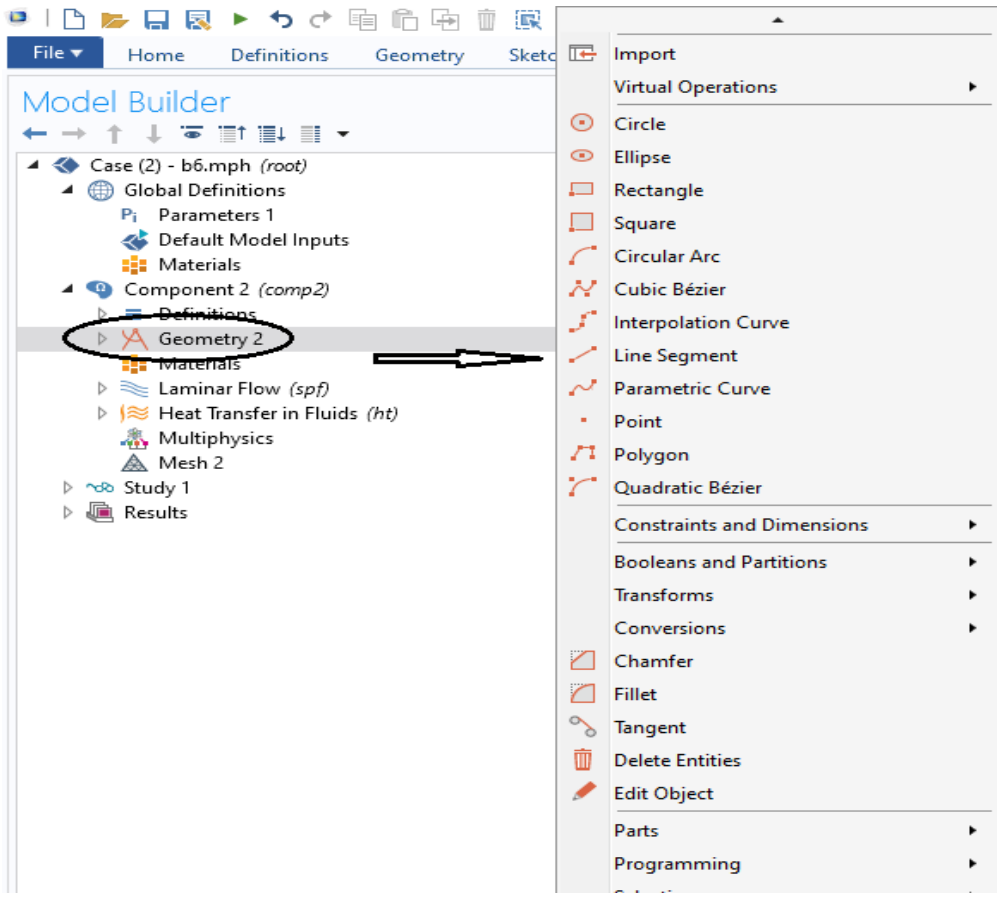

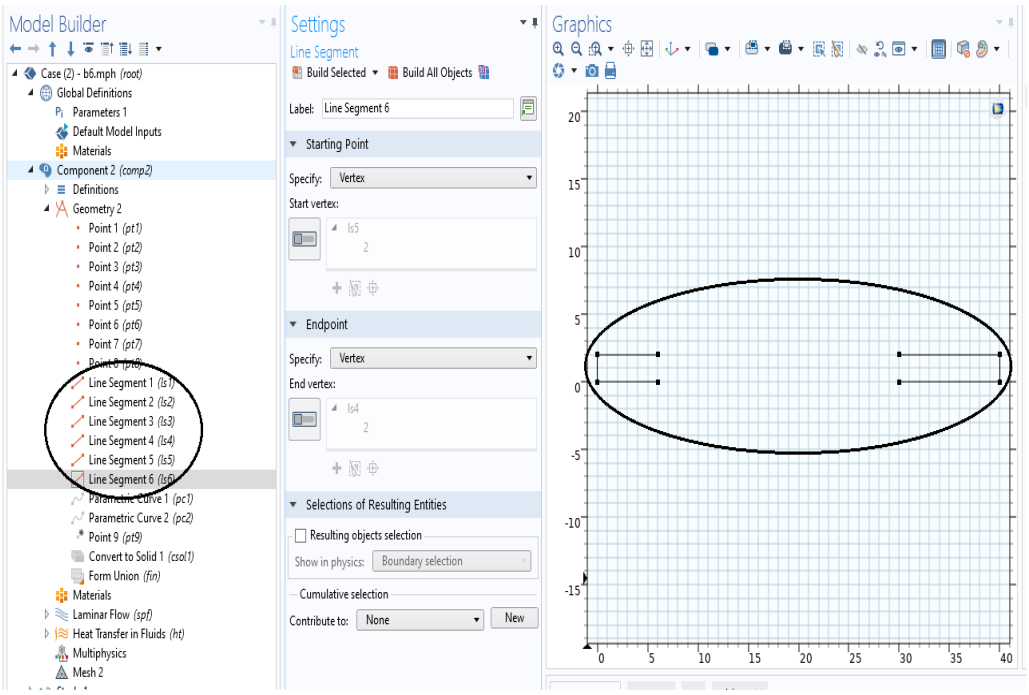

Figure (A- 8) draw line.

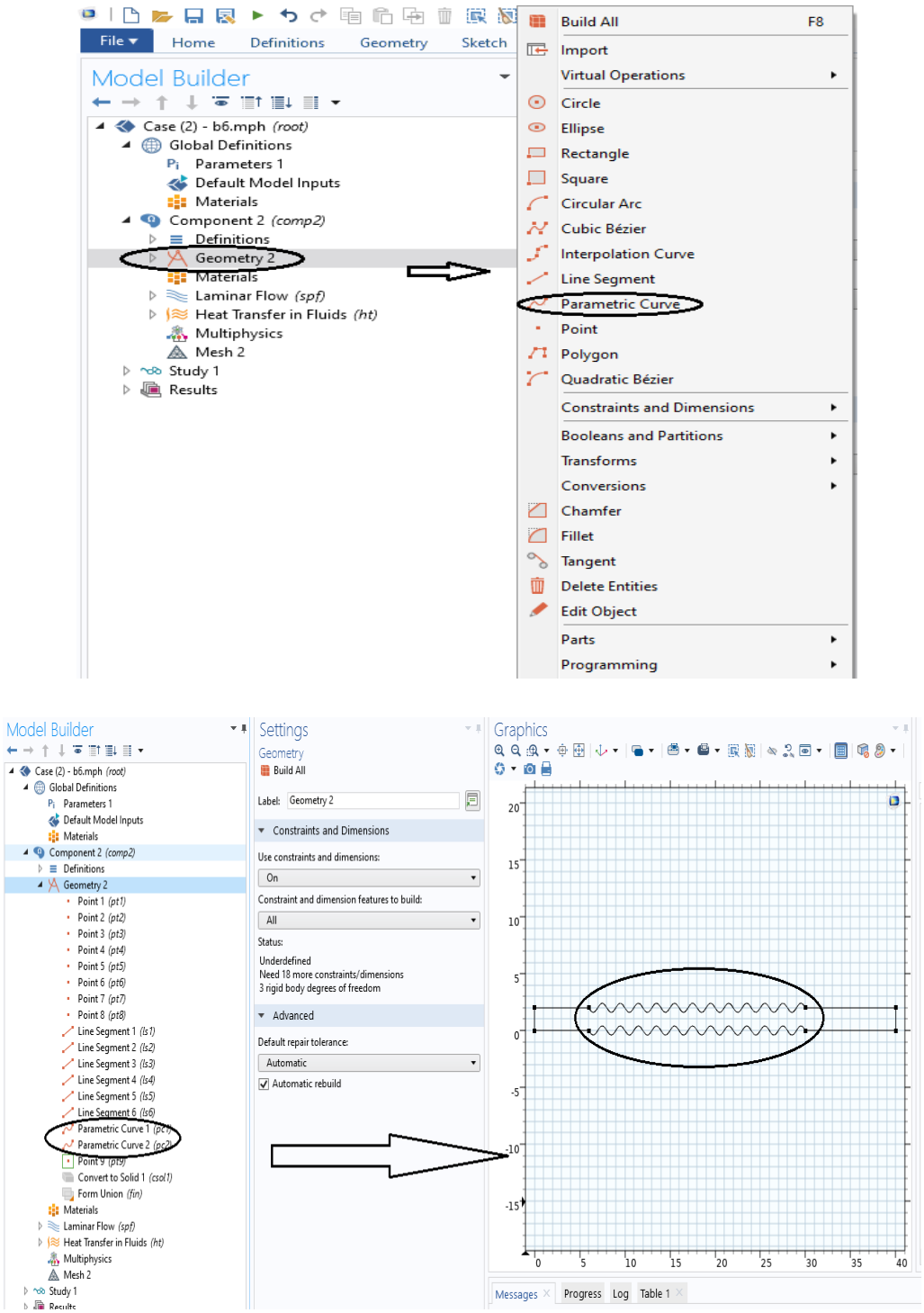

Figure (A- 9) draw parametric curve.

8-Setting the heat transfer and Laminar flow in the fluid and choose the fluid, initial values, inflow, out flow, wall temperature, fluid properties, no slip condition wall, and inlet and outlet.

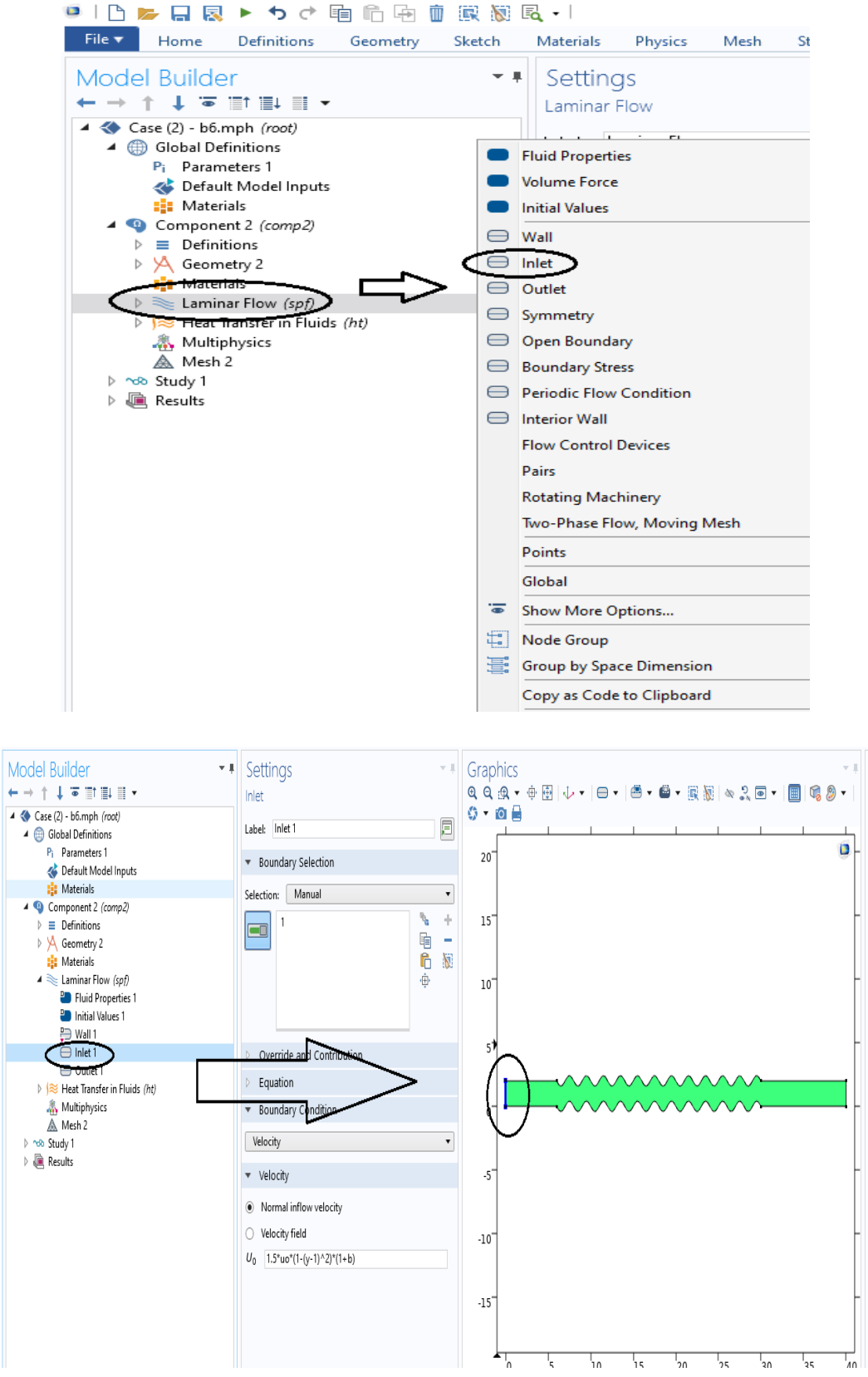

Figure (A- 10) insert inlet laminar flow.

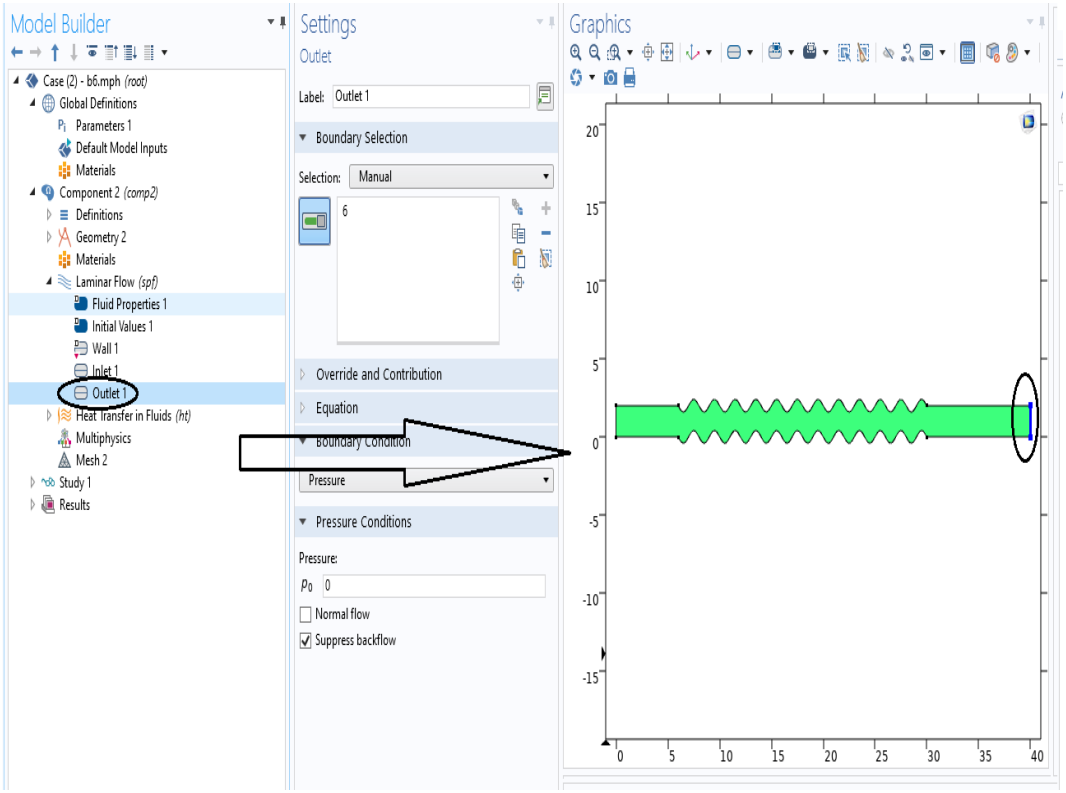

Figure (A- 11) insert outlet laminar flow.

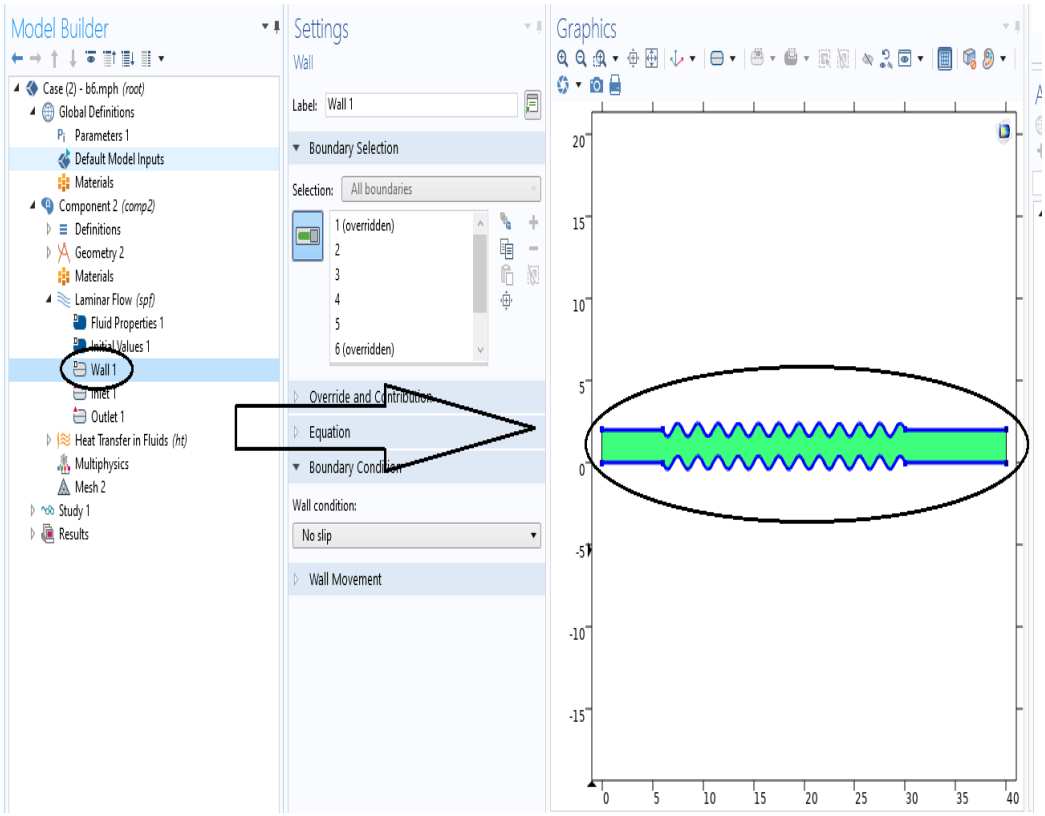

Figure (A- 12) select all the wall.

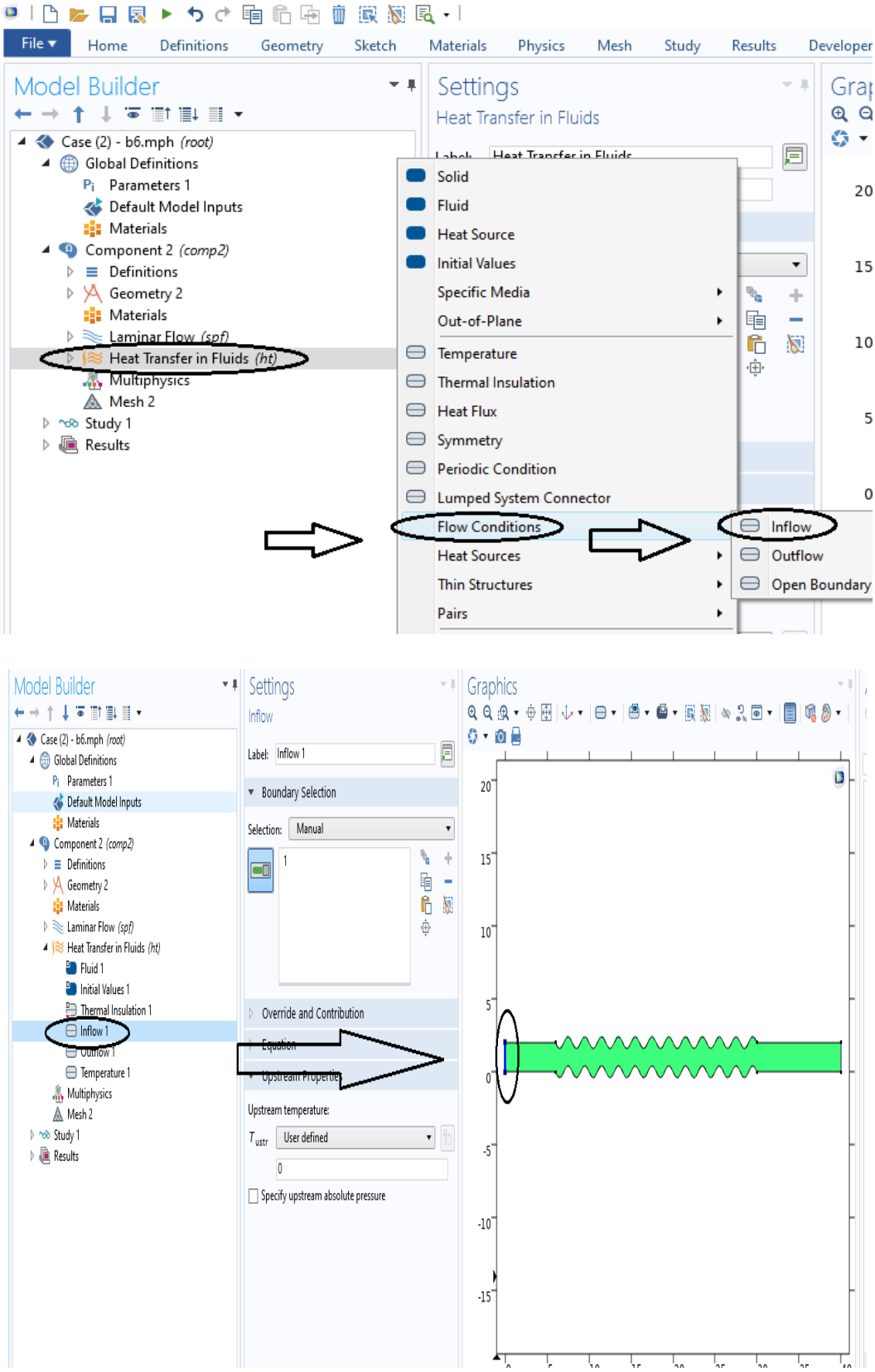

Figure (A- 13) insert inlet heat transfer.

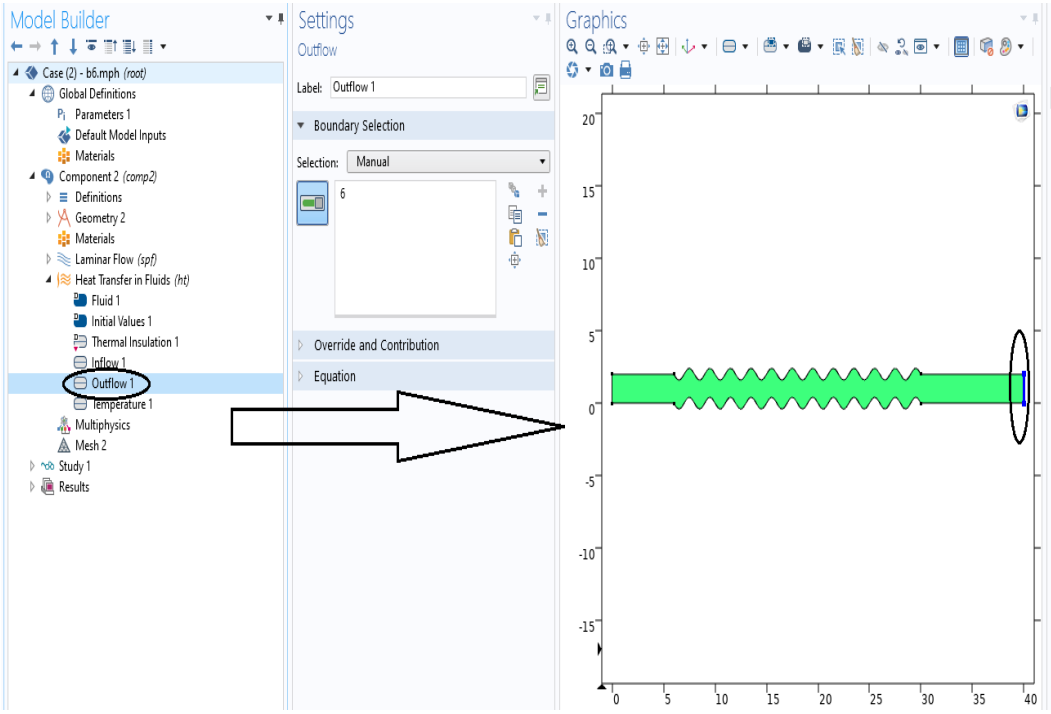

Figure (A- 14) insert outlet heat transfer.

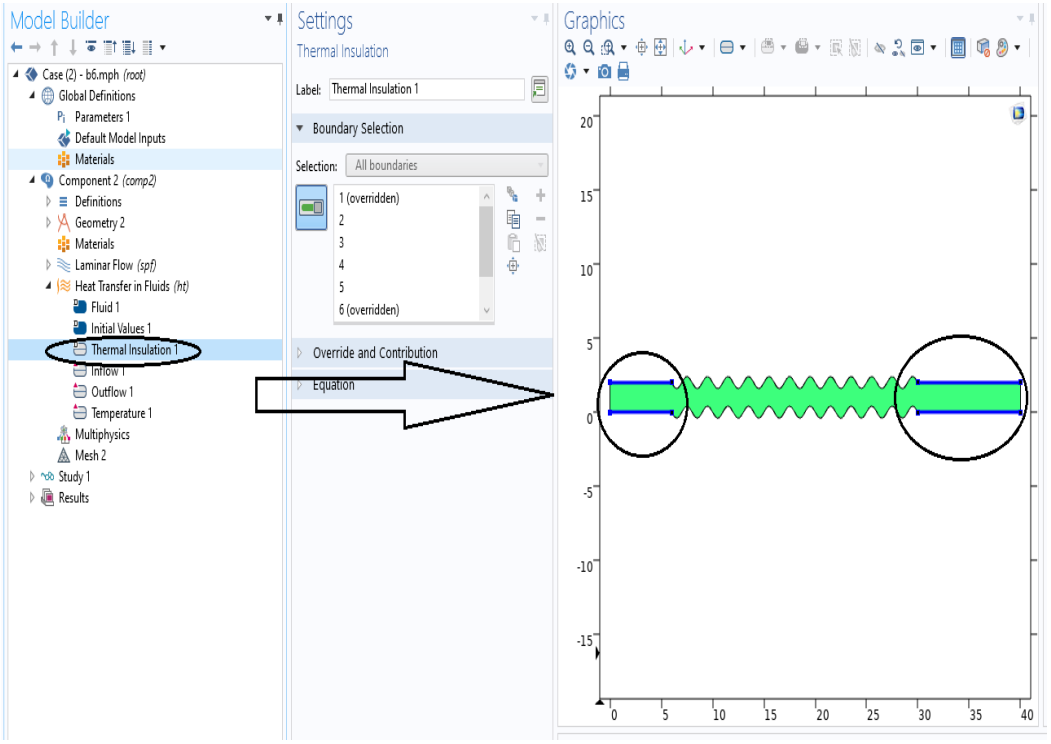

Figure (A- 15) select wall insulation.

8- Mesh the geometry.

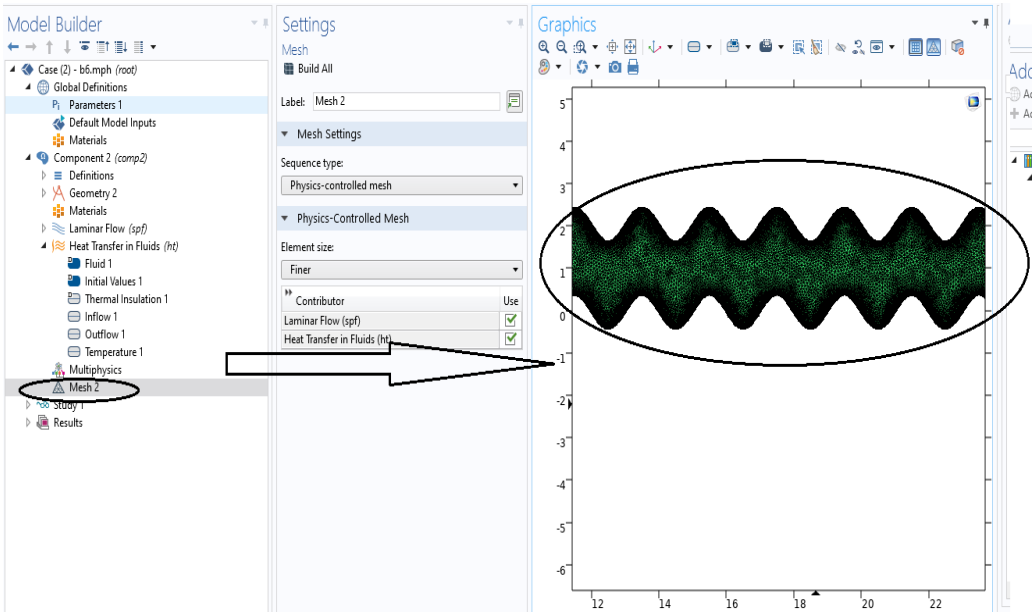

Figure (A- 16) insert mesh.

9- Study and computations the problem in varies Reynolds number (Re) at varies value of (Strouhal numbers **(**St), wavy number(β) and amplitude(α)).

10-The temperature, velocity, isothermal and stream line counters that the results from the program and then compute the Nusselt number (Nu).

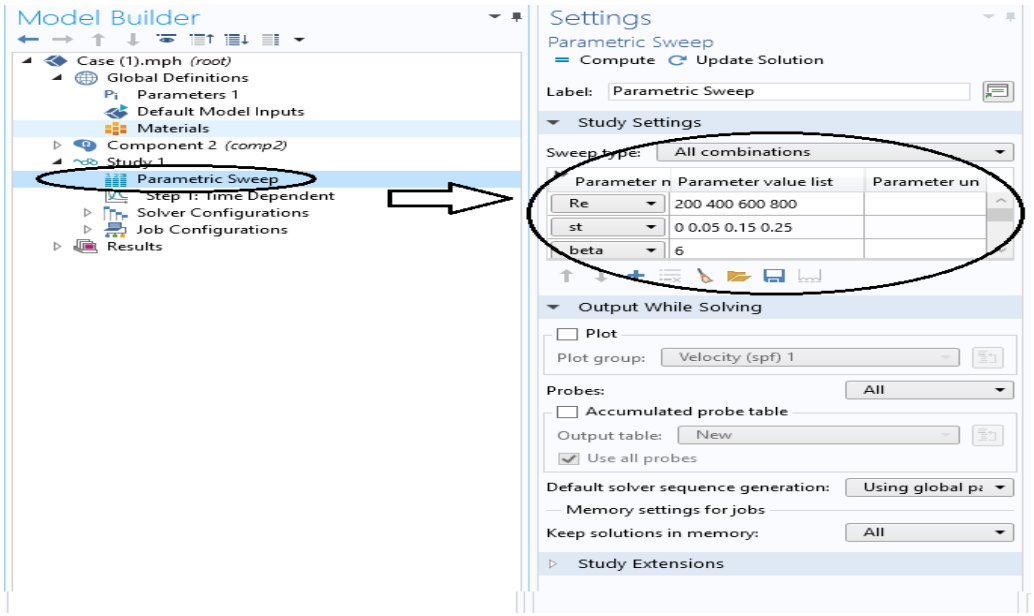

Figure (A- 17) insert parameter sweep.

الخلاصة

تمت دراسة انتقال حرارة لقود الكيروسين عدديًا داخل قنوات متوجة الشكل تحت تأثير التدفق النبضي. ركزت الدراسة على معرفة تأثير الوقود في كمية انتقال الحرارة اعتمادًا على الخصائص الفيزيائية للوقود في قناة المتموجة.

تم استخدام وحدة CFD في Comsol Multiphysics في دراستنا ، وقد استندت إلى طريقة العناصر المحدودة لحل المعادلات التفاضلية الجزئية التي تحكم مجال المشكلة (الاستمرارية ، والزخم ، والطاقة).تم استخدام عدة متغيرات في هذه الدراسة وتطبيقها على الوقود المستخدم حيث تم تطبيق عدة متغيرات على الجريان منها قيم رقم رينولز (200,400,800) وكذلك تم استخدام عدة قيم من رقم ستروهال (0,0.05,0.15) ،تم استخدام قيم مختلفة متغيرة على هيكل القناة المتموجة منها عدد التموجات (0,4,8) وكذلك قيم متغيرة من سعة الموجة (0,0.2,0.3).من خلال دراستنا الحالية استنتجنا انه يحصل تحسن في مقدار انتقال الحرارة للوقود المستخدم عند زيادة رقم ستروهال مع زيادة رقم رينولز حيث زيادته يؤدي الى زيادة (رقم نسلت) وهذا بدوره يؤدي الى التحسن في الانتقال الحراري.كذلك تم ملاحظة عند زيادة ابعاد القناة المتموجة حيث عند زيادة عدد التموجات تزداد المساحة السطحية للقناة وهذا بدوره يؤدي الى التحسن بقيم انتقال الحرارة حيث تم ملاحظة قيم (رقم نسلت =107.82) عند . (β=4, Re=800, α=0.2, St=0.15).حيث نلاحظ النسبة المئوية للتحسن عند هذه القيمة هي (1.53662) . بينما تصبح قيمة (رقم نسلت =124.26) عند نفس الخواص ولكن عند قيمة (عدد التموجات=8)، حيث نلاحظ النسبة المئوية للتحسن تصبح (1.923306). كذلك نلاحظ قيم التحسن الحراري في زيادة واضحة عند زيادة سعة الموجة لانه زيادة سعة الموجه كذلك يؤدي بدوره الى زيادة المساحة السطحية للقناة وهذا يؤدي الى زيادة قيم (رقم نسلت) والذي بدوره يحسن من انتقال الحرارة وبالتالي تصبح نسبة التحسن (2.663) عندما تكون قيمة (رقم نسلت= 146.2) عند سعة الموجة (α = 0.3) و (Re = 800).

جمهورية العراق
وزارة التعليم العالي والبحث العلمي
جامعة بابل / كلية الهندسة
قسم الهندسة الميكانيكية

تقصي الجريان النبضي في قناة متموجة مملوءة بوقود الكيروسين

بحث
مقدمة إلى كلية الهندسة – جامعة بابل وهي جزء من متطلبات نيل درجة الدبلوم العالي في الهندسة / الهندسة الميكانيكية/ وقود وطاقة

أعدت من قبل
امير كريم سلهو جراح

بأشراف

ا.م.د. حميد كاظم حمزة

2022 م